Design of HER2-specific Virus-Like Particles: the next step in targeted therapy

Joana Pinto dos Santos

Thesis to obtain the Master of Science Degree in

Biomedical Engineering

Supervisors:

Doctor Rita Lourenço Paiva de Melo

Doctor Sandra Isabel Silva Damas Cabo Verde

Examination Committee

Chairperson: Doctor Maria Margarida Fonseca Rodrigues Diogo

Supervisor: Doctor Rita Lourenço Paiva de Melo

Members of the Committee: Doctor Frederico Nuno Castanheira Aires da Silva

Doctor Joana Filipa Fernandes Guerreiro

July 2021

Preface

The work presented in this thesis was performed at the Centre for Nuclear Sciences and Technologies (C2TN) of Instituto Superior Técnico (Lisbon, Portugal), during the period February 2020-July 2021, under the supervision of Dr. Rita Lourenço Paiva de Melo and Dr. Sandra Isabel Silva Damas Cabo Verde.

Declaration

I declare that this document is an original work of my own authorship and that it fulfils all the requirements of the Code of Conduct and Good Practices of the Universidade de Lisboa.

Acknowledgements

I would like to acknowledge all the people directly or indirectly involved in this thesis.

Firstly, I would like to start by expressing my sincere gratitude to Dr Rita Melo for accepting me as a master thesis student at Centre for Nuclear Sciences and Technologies, Instituto Superior Técnico, Universidade de Lisboa, and for all the support, patience and kindness throughout this project and the useful teachings that improved my work.

I would also like to thank Dr. Sandra Cabo Verde for receiving me in her laboratory, and for all the help given in it, for all the support, insights, patience and kindness throughout this project.

Profound thanks go to Miguel Cardoso for his crucial contribution and inputs throughout this work. I am also deeply grateful for his knowledge transmission, tremendous dedication, help in this project and friendly words. I would also like to thank for all the material provided.

A special thanks to Dr. João Galamba for the inputs given to my work and the articles revision.

I would like to thank Dr. João Gonçalves for letting me use the facilities of the iMed ULisboa group and Dr. Filipa Mendes for allowing me to use the cell laboratory of the Radiopharmaceutical Sciences group,for the period when due to Covid the laboratory where I worked had to suffer some changes.

To all my laboratory colleagues, Joana Madureira, Inês Gonçalves, Jéssica Cardoso e Miguel Martins. Thank you for the help to see the light at the end of the tunnel.

I could not fail to highlight the Radiopharmaceutical Sciences group, in particular to Joana Guerreiro, Rúben Silva, Catarina Pinto, Salete Baptista and João Machado for all the help and friendship.

I would also like to acknowledge the technical facilities of the Radiation, Elements and Isotopes group, Radiopharmaceutical Sciences group as well as iMed ULisboa group for providing their equipment and services.

A huge thanks to my friends: Magda Carrilho, Claúdia Ferreira, Maria Fernandes, Rita Navega, Margarida Ruela, Rita Soares, Diana Oliveira and Nazaré Mangerona for their crucial support and availability in listening my concerns, and for giving me suggestions to improve and overcome obstacles. I greatly value your friendship and I deeply appreciate your belief in me.

Most importantly, none of this would be possible without the love and patience of my family, especially my mum, dad and brother. During my life, you were a constant source of love, strength and support. I could not have done this without you.

Abstract

In recent years, exciting new diagnosis and treatment strategies have emerged in the context of cancer research. Human Epidermal Growth Factor Receptor 2 (HER2) positive cancers are extremely aggressive, associated with a poor prognosis and are most commonly treated with trastuzumab. However, not all patients respond to this therapy. Virus-like particles (VLPs) arise as promising nanoplatforms to be used as drug delivery systems. They can acquire specificity through the expression, on their surface, of a cell target-specific molecule of interest, increasing the therapeutic efficacy of a drug.

The main goal of this thesis was the development and characterization of an HIV-1 based VLP containing on the surface a single chain variable fragment (scFv) of an anti-HER2 antibody. The mammalian HEK-293T cell line was chosen to produce the HIV-1 based VLPs by transient transfection. *In vitro* studies were done to assess the presence of the fusion protein, binding to the HER2 target and the cytotoxic effects of VLPs. Our results showed the efficient production of HIV-1 based VLPs containing on the surface a scFv of an anti-HER2 antibody. More importantly, the preliminary results obtained indicated binding between the receptor HER2 and engineered HIV-1 based VLP, highlighting that trastuzumab scFv when expressed on the VLP surface maintains its specificity to HER2. No cytotoxicity was detected after incubating the SK-BR-3 cells with the HIV-1 based VLPs produced. This work can be the kick-off for new approaches towards targeted therapies for HER2 overexpressing cancers and anti-HER2 delivery systems.

Keywords

HIV-1 based Virus-like Particles; Human Epidermal Growth Factor Receptor 2 (HER2); Target Therapy; Therapeutic Delivery System; HER2-specific Virus-like Particles.

Resumo

Recentemente, surgiram novas estratégias de diagnóstico e tratamento na investigação sobre o cancro. O recetor para o fator de crescimento epidérmico tipo 2 (HER2) quando expresso em excesso torna os casos de cancro extremamente agressivos e com baixo prognóstico de cura, sendo normalmente tratados com trastuzumab. Contudo, nem todos os doentes respondem a esta terapia. As partículas semelhantes a vírus (VLPs) surgem como promissoras nanoplataformas para serem usadas como sistemas de administração de medicamentos. Elas podem adquirir especificidade expressando, na sua superfície, uma molécula específica da célula alvo, aumentando a eficácia terapêutica.

O objetivo desta tese foi o desenvolvimento e caracterização de uma VLP baseada no VIH-1 que contém na sua superfície um fragmento variável de cadeia simples (scFv) de um anticorpo anti-HER2. A linha celular de mamífero HEK-293T foi escolhida para produzir as VLPs por transfeção transitória. Foram realizados estudos *in vitro* para avaliar a presença da proteína de fusão e a sua ligação ao alvo HER2 bem como os efeitos citotóxicos das VLPs. Os resultados mostraram uma produção eficiente de VLPs baseadas no VIH-1 contendo na sua superfície a scFv de um anticorpo anti-HER2. Mais importante ainda, os resultados preliminares obtidos, mostraram ligação entre o recetor HER2 e a VLP destacando que manteve-se a especificidade do trastuzumab scFv quando expresso na superfície da VLP. Não foi detetada citotoxicidade nas células SK-BR-3 quando incubadas com as VLPs. Este trabalho pode iniciar novas abordagens nas terapias direcionadas para cancros que expressam em excesso o HER2 e sistemas de administração anti-HER2.

Palavras-Chave

Partículas semelhantes a vírus baseadas no VIH-1; Recetor para Fator de Crescimento Epidérmico tipo 2 (HER2); Terapia Direcionada; Sistema de Administração Terapêutica; Partículas semelhantes a vírus específicas para o HER2.

Contents

List of Figures

List of Tables

List of Abbreviations

ADCC	Antibody-dependent cellular cytotoxicity
BSA	Bovine serum albumin
CA	Capsid
CT	Cytoplasmic tail
DMEM	Dulbecco's modified Eagle's medium
DNA	Deoxyribonucleic Acid
EGE	Extended gene expression
ELISA	Enzyme-linked immunosorbent assay
Env	Envelope
Fab	Fragment antigen-binding
FSC	Forward scatter
GFP	Green Fluorescence Protein
gp120	Glycoprotein 120
gp41	Glycoprotein 41
h	Hours
HA	Hemagglutinin
HBV	Hepatitis B Virus
HEK-293	Human Embryonic Kidney-293
HER2	Human Epidermal Growth Factor Receptor 2
HIV	Human Immunodeficiency Virus
HIV-1	Human Immunodeficiency Virus-1
HPV	Human Papillomavirus
HRP	Horseradish peroxidase
IgG	Immunoglobulin G
Kan	Kanamycin

LB	Luria-Bertani Broth
MA	Matrix
mAb	Monoclonal antibody
MAPK	Mitogen-activated protein kinase
MEM	Minimum Essential Medium
min	Minutes
mRNA	Messenger RNA
NC	Nucleocapsid
P13K	Phosphatidylinositol 3-kinase
PBS	Phosphate-buffered saline
PCR	Polymerase chain reaction
RNA	Ribonucleic acid
rpm	Revolutions per minute
scFv	Single chain variable fragment
SDS-PAGE	Sodium dodecyl sulfatepolyacrylamide electrophoresis
shRNA	Short hairpin RNA
siRNA	Small interference RNA
SSC	Side scatter
TEM	Transmission electron microscopy
TSB	Tryptic Soy Broth
VLP	Virus-like particle
WST-1	Water Soluble Tetrazolium-1

1. Introduction

1.1. Human Epidermal Growth Factor Receptor 2

Human Epidermal Growth Factor Receptor 2 (HER2) also known as ErbB2 is a 185 kDa glycoprotein, constituted by an intracellular tyrosine kinase domain, a transmembrane domain and an extracellular ligand binding domain (Advani et al., 2015). HER2 mediates several signalling pathways important to promote cell proliferation and prevent apoptosis, such as mitogen-activated protein kinase (MAPK) pathway and phosphatidylinositol 3-kinase (P13K) pathway (Tai et al., 2010; Dhritlahre & Saneja, 2021).

HER2 is also involved in cell growth, differentiation, and survival (Iqbal & Iqbal, 2014). Due to its functions, when the *HER2* gene is amplified, the protein will be overexpressed, which can cause a malignant cellular formation (Figure 1). There is a direct association between this and a poor clinical outcome in breast, gastric, ovarian, and prostate cancer, among other cancers.

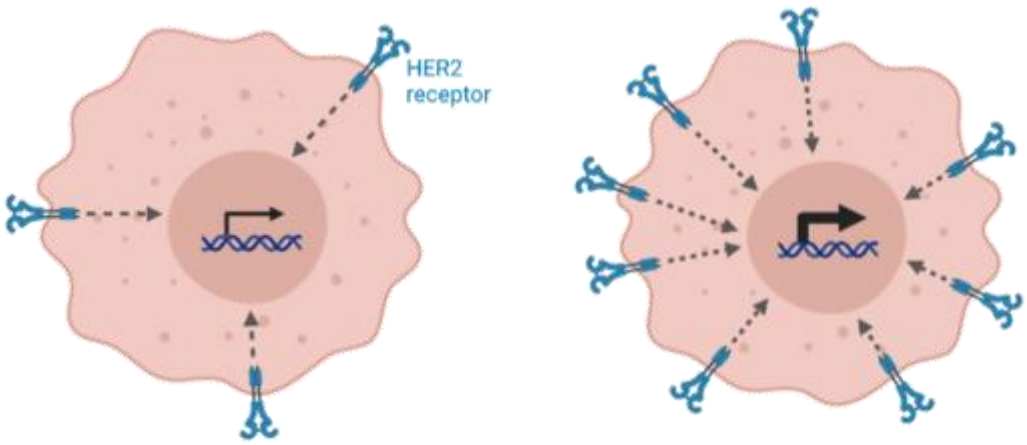

Figure 1: Left- Heathy cell, where HER2 receptor sends signals for cells to grow and divide. Right- HER2 positive cancer cell, where there is an overexpression of HER2 receptors, causing tumorigenesis. Adapted from a BioRender template.

Hence, the scientific and medical communities have shown interest in finding therapeutic solutions to inhibit HER2 positive cells. An anti-HER2 antibody was successfully developed, trastuzumab (Herceptin™) (Han-Chung et al., 2006; Tan & Swain, 2003), which had a huge influence on breast

cancer treatment (Figure 2). This breakthrough was the initial step for new studies where the HER2 receptor and HER2 signalling pathways are used as targets for cancer therapy. HER2 is a potential marker for targeted drug delivery, due to its overexpression in tumour cells.

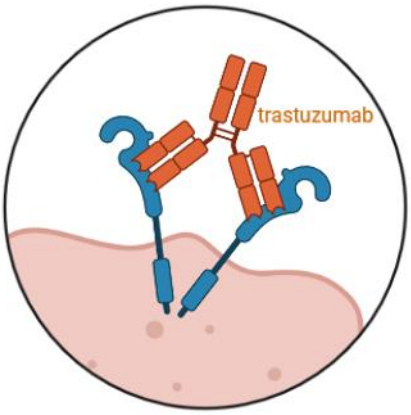

Figure 2: Trastuzumab targets the HER2 receptor and can block its dimerization, which will inhibit several signalling pathways that stimulate abnormal cell growth. Adapted from a BioRender template.

1.1.1. Pathologies associated with HER2

While in healthy cells HER2 participates in all phases of cell development, when there is overexpression of this protein or a mutation, it can induce tumorigenesis or metastasis. *HER2* overexpression is common in breast, gastric and ovarian cancers (Tai et al., 2010).

1.1.1.1. Breast cancer

Breast cancer cells that overexpress *HER2* are present in approximately 15%–30% of all diagnosed breast cancers. This type of breast cancer is extremely aggressive, has a poor prognosis, and can become therapy/drug resistant. It is also associated with significantly shorter relapse times and overall survival (Advani et al., 2015; Dai et al., 2017). HER2 has a crucial role in the proliferation and anti-apoptosis of HER2 positive breast cancer.

Several studies propose that *HER2* overexpression inhibition induces apoptosis of breast cancer cells (Faltus et al., 2004; Yang et al., 2004), highlighting the crucial role of HER2 as a target for breast cancer therapy.

For HER2 positive tumours, the most used antibody is trastuzumab, a humanized monoclonal anti-HER2 antibody that induces apoptosis in breast cancer cells through antibody-dependent cellular cytotoxicity (ADCC) (Dhritlahre & Saneja, 2021). However, not all HER2 positive patients respond to this therapy. Some *HER2* overexpressing tumours develop intrinsic resistance to trastuzumab

monotherapy. In contrast, combined therapy of trastuzumab along with other anti-cancer drugs such as paclitaxel, docetaxel, lapatinib and anthracyclin provides a better and complete therapeutic effect (Tai et al., 2010). All of these treatments are usually associated with chemotherapy.

1.1.1.2. Gastric cancer

Gastric cancer that overexpresses *HER2* is present in approximately 6%–35% of all diagnosed gastric cancers. It is associated with a poor prognostic. Trastuzumab is also an effective therapy in this type of cancer, prolonging the overall survival when combined with chemotherapy (Tai et al., 2010).

1.1.1.3. Ovarian cancer

It is estimated that 9%–32% of all diagnosed ovarian cancers overexpress *HER2*. This kind of cancer is less studied than other types, but it seems that *HER2* overexpression is more prevalent in advanced stages of ovarian cancer (Tai et al., 2010).

In ovarian cancer cells, the overexpression of HER2 induces a faster cell growth, higher abilities in DNA repairment and colony formation. The oestrogen induces HER2 phosphorylation and initiates its signalling pathway (Tai et al., 2010).

1.1.1.4. Prostate cancer

Although *HER2* is not overexpressed in prostate cancer cells, treatments with trastuzumab have shown a small effect in advanced hormone-refractory prostate cancer (Ziada et al., 2004). Prostate cancer recurrence occurs when there is a reactivation of the androgen receptor that causes cancer cells growth (Liu et al., 2005). HER2 activates the androgen receptor through the MAPK pathway. For this reason, HER2 may become a therapeutic target for aggressive hormone-refractory prostate cancer.

1.1.2. HER2 in cancer therapy

HER2 is a vital therapeutic target for cancer therapy. The reasons for this role are firstly that the upregulation of HER2 levels induces tumorigenesis in cancer cells, in which *HER2* gene expression is increased when compared with healthy cells. Secondly, primary tumours and metastasized organs also overexpress *HER2* (Niehans et al., 1993). Furthermore, the activation of MAPK and P13K pathways that may cause carcinogenesis, can be inhibited if HER2 dimerization does not happen (Franklin et al., 2004; Nahta et al., 2006). In addition, all domains of HER2 are responsible for a specific aspect of its

signalling pathways, which means they can be targeted on their own to block the HER2 signalling (Niehans et al., 1993).

The activation of HER receptors, due to HER2 dimerization with other HER receptors, causes cell growth, proliferation, decreased apoptosis, cellular migration and angiogenesis. In order to supress this dimerization, monoclonal antibodies targeting HER2 extracellular domain can be used. The inhibition of HER2 dimerization can stop several signalling pathways associated with HER2 dimers.

Trastuzumab is an antibody that targets HER2 extracellular domain. It shows therapeutic value in *HER2* overexpressing metastatic and early-stage breast cancer (Nahta et al., 2006; Cameron & Stein, 2008). Pertuzumab is a recombinant humanized monoclonal antibody that inhibits HER2 dimerization (Agus et al., 2002, 2005).

Another target in the HER2 signalling pathway is its intracellular domain. Preventing the phosphorylation of the tyrosine kinase domain can slow down the initiation of this pathway.

Lapatinib is a small molecular inhibitor of HER2 intracellular domain. This molecule stops the signal transduction from HER2 receptors, which will inhibit the growth of tumours overexpressing *HER2* (Rusnak et al., 2001; Reid et al., 2007).

HER2 gene expression can be repressed by oligonucleotides, such as antisense oligonucleotide and siRNA. Antisense oligonucleotides bind to the complementary mRNA sequence of *HER2* inducing its degradation, which prevents the proliferation of *HER2* overexpressing cancer cells (Roh et al., 1999, 2000). siRNA also degrades the mRNA through a RNA interference mechanism (Tai et al., 2010). Inhibition of *HER2* expression by this mechanism leads to an increase in apoptosis, a reduction on proliferation, and an inhibition of tumour growth in breast and ovarian tumour cells overexpressing *HER2* (Yang et al., 2004).

1.1.3. HER2 in targeted drug delivery

Targeted therapies are a new generation of cancer drugs that block the growth and proliferation of cancer cells by interfering with specific target proteins that play a crucial role in tumour growth or progression (Wu et al., 2006; Gerber, 2008). These novelty therapies can overcome the lack of specificity of the conventional cancer therapies and reduce the toxicity to off-target cells (Padma, 2015). The development of targeted therapies requires the identification of a differential expressed target specific for the cancer cell, also known as a cancer marker (Y. T. Lee et al., 2018).

HER2 can be used as a marker for receptor mediated targeted drug delivery system, because this receptor is upregulated in cancer cells and has an accessible extracellular domain (Lewis Phillips et al., 2008). Due to the lack of a HER2 natural ligand, artificial ligands were developed for HER2 targeted

drug delivery, such as HER2 specific antibodies or fragments, affibodies and peptides. These ligands have to have high affinity and be stable in the blood circulation.

The properties of the different artificial anti-HER2 ligands are presented in Table 1.

Table 1: Properties of the different artificial anti-HER2 ligands. Adapted from (Tai et al., 2010).

Properties	Antibody	Fab	scFv	Affibody	Peptide
Molecular Weight	150 kDa	55 kDa	27 kDa	5-6 kDa	~1 kDa
Immunogenicity	Yes	No	No	No	No
Ligand affinity (Kd)	pM-nM	nM	nM	nM-µM	µM
$T_{1/2}$*	2-3d	~4h	30-60min	10-60min	~5min
Tissue penetration ability	Poor	Moderate	Moderate	Good	Excellent

*in nude mice blood

One of the most studied ways of drug delivery is through specific transporters as nanoparticles and immunoliposomes (Tai et al., 2010). When the target is HER2, the surface of these systems can be modified with anti-HER2 antibodies or its fragments (Fab or scFv) to identify overexpressing *HER2* cancer cells. They may be used to deliver therapeutic drugs (Park et al., 2002). These anti-HER2 delivery systems increase the therapeutic index by enhancing the anti-tumour efficacy and reducing the systemic toxicity.

Affibody molecules are small and stable platforms derived from the IgG binding domains of staphylococcal protein A. This ligand can be used for targeted drug delivery and tumour imaging, due to its size (6 kDa) and its ability to penetrate the cells (Table 1). In addition, its binding site is distanced from its functional end groups. It can also be produced in large-scale (Alexis et al., 2008). Affibodies have a short plasma circulation and fast blood clearance, making them ideal for imaging, but not as therapeutic delivery systems (Tolmachev et al., 2007).

Finally, among the different types of anti-HER2 ligands (Table 1) are peptides. These structures are molecules with low molecular weight (~1 kDa), with great cell penetration, which are easy to produce and flexible in chemical conjugation, making them a suitable targeting moiety (Table 1) (Tai et al., 2010; Sanna et al., 2014).

1.2. Virus-like particles

Virus-like particles (VLPs) are multiprotein biological entities that mimic the structure of their corresponding wild-type virus. They are nanoparticles constituted by self-assembled viral capsid proteins, also known as capsomeres (Pumpens & Grens, 2002; Forouhar-Kalkhoran, 2017). VLPs have a stable structure and are functionally versatile, which makes them ideal for a variety of scientific developments in the medicine area, such as vaccines and as delivery vehicles for therapeutic and/or imaging agents (Lua et al., 2014; Mohsen et al., 2017).

VLPs are non-infectious since they do not contain any of the virus genetic material and are unable to replicate, bringing no safety concerns when administrated. Despite the absence of the virus genetic material, they still maintain the tropism and antigenicity characteristic of the native virus (Lua et al., 2014; Zdanowicz & Chroboczek, 2016; Forouhar-Kalkhoran, 2017).

Upon heterologous expression in a host system, the proteins can self-assemble and form VLPs, which can then be purified from the cells or the cell culture supernatant.

1.2.1. Physicochemical properties of VLPs

VLPs are multimeric nanostructures that have a size range from 20 to 200 nm (Manolova et al., 2008; L. A. Lee et al., 2009; Mohsen et al., 2017).

They can be built from proteins of a single virus, or structural proteins from different viruses forming chimeric VLPs (Zdanowicz & Chroboczek, 2016). VLPs can form icosahedral, spherical or rod-shape (helical) structures by the self-assembly of these viral structural proteins, depending on the type of the original virus (Mohsen et al., 2017).

These nanostructures can be classified as enveloped or non-enveloped depending on the presence of a lipid envelope (Chroboczek et al., 2014; Zdanowicz & Chroboczek, 2016). The lipid membrane of the enveloped VLPs derives from the host cell during the assembly and budding of the VLPs protein capsid. Functionalising enveloped VLPs is easier than non-enveloped VLPs due to the presence of the lipid membrane (Forouhar-Kalkhoran, 2017). Enveloped VLPs are more environmentally sensitive than non-enveloped VLPs. Their integrity and stability can be compromised by purification processes, sample handling and temperature variations, which can lead to a reduction in immunogenicity (Nooraei, et al, 2021).

VLPs can also be categorized based on how the capsid proteins are arranged: one, two or three layers, or as single-protein and multi-protein VLPs. Single-protein VLPs have a simple structure constituted only by a single layer, while multi-proteins can have several capsid layers (Lua et al., 2014; Nooraei et al, 2021).

VLPs can comprise viral surface proteins responsible for virus cell penetration, which provides the efficient ability of cell entry and consequently allows for tissue-specific targeting (Beyer et al., 2001; Zdanowicz & Chroboczek, 2016). This makes it possible to engineer VLPs to encapsulate proteins, peptides, nucleic acids or even imaging compounds, pharmaceutical drugs, quantum dots and other types of nanoparticles (Pokorski & Steinmetz, 2011; Lua et al., 2014). VLPs are also able to be internalized through simple diffusion, in different systems of the human body, particularly into the lymphatic system due to their size (Manolova et al., 2008; L. A. Lee et al., 2009; Mohsen et al., 2017).

Several studies propose that VLPs have a high-immune response-stimulating activity, inducing a strong humoral and cellular immune response (Shirbaghaee & Bolhassani, 2016; Caldeira et al., 2020). Their use can lead to B cell activation through increased antibody production due to the densely repeated, structured VLP surface amino acid motifs. The uptake of VLP and its consequent degradation by antigen-presenting cells leads to T cell activation. These behaviour together with the lack of viral genome, which hinders replication within the target cell, makes VLP a relevant candidate to replace conventional therapeutics (M F Bachmann et al., 1993; Martin F Bachmann & Zinkernagel, 1997; Beyer et al., 2001; Martin F Bachmann & Dyer, 2004; J. W. Wang & Roden, 2013; Zeltins, 2013).

VLPs have all the desirable characteristics necessary for a biological vector: biocompatibility, solubility, uptake efficiency, target delivery and high drug loading capacity (Yan et al., 2015). However, their high immunogenicity can induce undesirable effects in the immune response of the patient to the drug delivery system. There are different nanoplatforms that have also been studying such as liposomes. Liposomes are biocompatible and have target delivery, high drug load capacity and a versatile structure (N. Wang et al., 2019). They also allow the purification of the envelope proteins prior to their formation (Brouwer & Sanders, 2019). Nevertheless, liposomes are less well defined than VLPs regarding drug delivery systems (Charlton Hume & Lua, 2017).

1.2.2. Platforms for VLP production

The selection of the most adequate expression system for the design of a VLP is a crucial step. Different expression platforms result in different protein folding and subsequent viral capsid quaternary structure. Expression systems include prokaryotic (bacteria) cells, eukaryotic (yeast, mammalian, insect, plant) cells and cell-free platforms, each with its own benefits and drawbacks.

As regards prokaryotic systems, bacteria are the most common recombinant protein expression platform. However, for VLP production, these systems are not the most commonly used. Owing to protein incompatibilities, incomplete disulphide bond formation and the lack of post-translational modifications, bacteria-based systems (e.g. *Escherichia coli*) are best suited for the expression and production of non-enveloped VLP (Nooraei et al, 2021).

Yeast systems have also been successfully used for VLP production. *Saccharomyces cerevisiae* and *Pichia pastoris* are widely used, due to rapid cell growth rates, high protein expression levels, good

production-cost ratios and scalability (Nooraei et al, 2021). Although recommended for non-enveloped VLP production, there have been reports of successful expression of HIV-1 Gag protein VLPs (McKinstry et al., 2014).

In contrast to prokaryotic systems, mammalian platforms execute precise and complex post-translational modifications, essential to protein folding. This makes them extremely efficient and appealing expression systems for both enveloped and non-enveloped VLPs. Efficient production of HIV- 1 based VLPs have been reported for HEK-293 and CAP-T cells. However, these systems have low production yields, long expression times, high production costs, product impurities from host cell debris and limited scalability, hindering its applications in pharmaceutical and industrial production (Nooraei et al, 2021).

Insect cell systems combine the high protein expression of prokaryotic systems with the complexity of post-translational modifications of mammalian cells to VLP production. However, the need for fresh batches for each individual production and product contamination with baculovirus-related proteins represent a major disadvantage of these systems (Lynch et al., 2010; Fernandes et al., 2020; Puente-Massaguer et al., 2021).

Plant cell systems have high expression yields and low maintenance costs. Plant cells as a production platform have major advantages: the matrix used does not need to be sterile and the bulk biomass production is significantly cheaper than in other production methods. This approach has successfully been used to produce various antigens and VLPs (Rybicki, 2019; Nooraei et al, 2021).

Cell-free systems rely on bacterial or yeast cells for the expression of the capsid proteins, while the VLP assembly is performed spontaneously in a cell-free environment (Zeltins, 2013). This system has high protein expression yields and product purity/homogeneity (Le & Müller, 2021; Nooraei et al, 2021). However, these *in vitro* expression systems have elevated production cost and poor scalability (Nooraei et al, 2021).

1.2.3. VLPs applications

Several studies show numerous applications for the VLPs, such as therapeutic delivery systems, imaging systems and for vaccines development.

1.2.3.1. Therapeutic delivery systems

Virus-based nanocarriers are promising novel platforms for the development of targeted therapeutic delivery systems. Besides improving on the physicochemical properties of the carried drug, these smart nanocarriers can release their therapeutic cargo in response to changes in the biological environment,

such as temperature, pH, osmotic pressure, calcium concentration, oxidative stress or other stimuli (Ma et al., 2012; van Kan-Davelaar et al., 2014; Zdanowicz & Chroboczek, 2016; Forouhar-Kalkhoran, 2017). During therapy, the ability to specifically target the desired cells, tissue or organ, reducing drug non-specificity and secondary effects while protecting drug stability and activity, is a highly desired characteristic for therapeutic carriers (Zdanowicz & Chroboczek, 2016).

1.2.3.2. Imaging systems

Imaging tools are powerful medicinal assets that allow the diagnosis, monitoring of various diseases and treatment response. Combining the carrier aspect of VLPs with an adaptable membrane, these nanocarriers become suitable tools for theragnostic (Bednarska et al., 2020; Y. Wang et al., 2020).

Labelling of VLPs can be achieved by various routes and with various imaging agents. By modifying the membrane external layer, these carriers can be functionalized with fluorescent proteins or radioisotopes (Flexman et al., 2008; Hooker et al., 2008; Bednarska et al., 2020). VLPs can also be designed to incorporate fluorescent cores and metallic nanoparticles through encapsulation. This permits the vessel to carry the imaging agent while leaving the external particle surface free for further modifications (Aljabali et al., 2020; Bednarska et al., 2020; Min et al., 2021).

Due to their characteristics as carriers, their protected, hollow core and designable membrane, VLPs represent highly suitable tools in the emerging field of disease theragnostic.

1.2.3.3. Vaccines

VLPs, due to their strong immunogenicity, are used in the development of recombinant vaccines and even as therapeutic vaccines (Yan et al., 2015). They can efficiently stimulate both humoral and cellular immunity (Shirbaghaee & Bolhassani, 2016; Caldeira et al., 2020). These VLPs are a safe alternative to inactivated vaccines or attenuated vaccines that generally induce side effects in the administered population (Kushnir et al., 2012).

Several VLP-based vaccines are under clinical trials and some have been approved, by the health authorities, and are already commercialized. The recombinant vaccines that are on the market are Gardasil® (human papillomavirus [HPV]), Gardasil® (HPV) and Recombivax HB® (HBV) from Merk, Cervarix® (HPV), Engerix® (hepatitis B virus [HBV]) and Mosquirix™ (malaria) from GlaxoSmithKline (GSK)'s Inc and Sci-B-Vac™ (HBV) from VBI Vaccines (Kushnir et al., 2012; Nooraei et al., 2021).

1.3. HIV-1 based virus-like particles

HIV-1 based VLPs are complex nanostructures that can be constituted by an internal structural protein, a lipidic membrane and envelope proteins (Figure 3). The core is formed by Gag polyproteins (García et al., 2021). The easy expression of *gag*, the stability and structure of these VLPs makes them a robust platform to be used in the development of recombinant vaccines and as delivery systems (Cervera et al., 2019). These VLPs can be functionalized through envelope glycoproteins with specific antigens (García et al., 2021; Lavado-García et al., 2021).

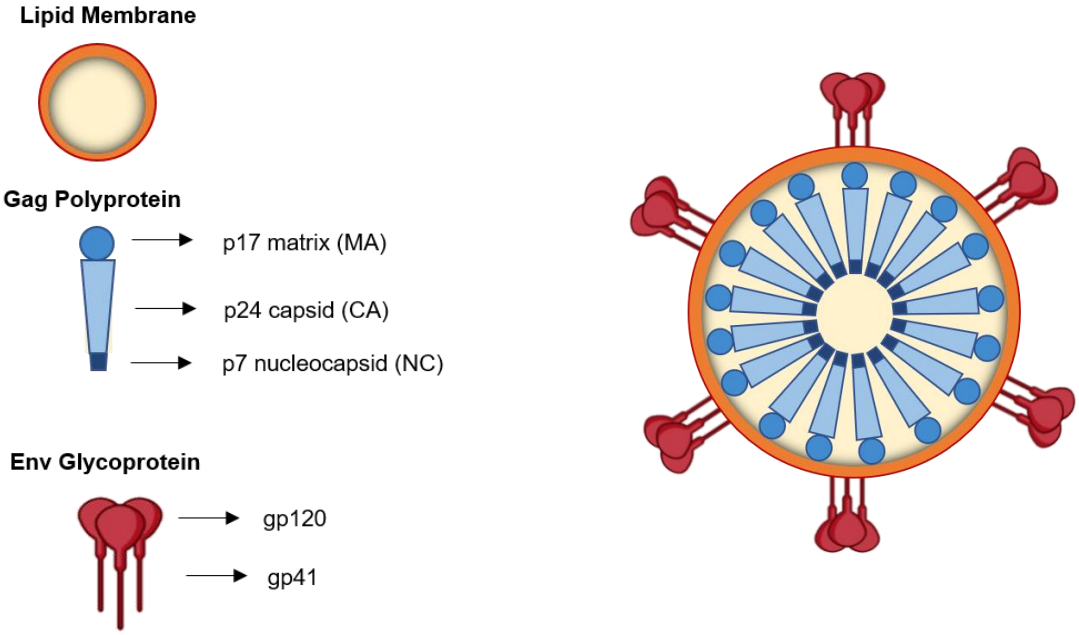

Figure 3: Schematic representation of an HIV-1 based VLP.

Two types of HIV-1 based VLPs can be formed. If the host cell expresses only the *gag* gene, a Gag-VLP (Figure 4), that resembles immature HIV virions, will be produced. If the *env* gene is co-expressed with *gag*, then a Gag-Env VLP (Figure 3) will be assembled and these envelope proteins will be present on the VLP surface (Buonaguro et al., 2013).

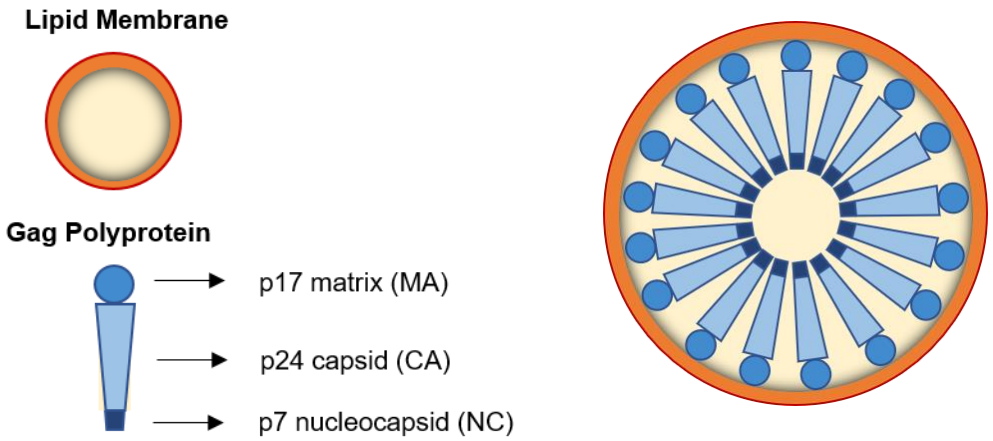

Figure 4: Schematic representation of an HIV-1 Gag VLP.

HIV-1 based virus-like particles are enveloped VLPs with a spherical structure. They are formed by an electrodense material that corresponds to the Gag capsid. The size of these particles is around 150 nm (Benjamin et al., 2005; Perlman & Resh, 2006; Gutiérrez-Granados et al., 2013; González-Domínguez et al., 2016; Lavado-García, Jorge, et al., 2021).

The model candidate presented in this thesis is a VLP formed by the HIV-1 Gag polyprotein and an envelope protein (Annexes_Figure A1) that translates a scFv from trastuzumab (anti-HER2 antibody fragment) fused with gp41 from HIV. The expression of this VLP in a mammalian system, the HEK-293T cell line, produces the VLP model present in Figure 5.

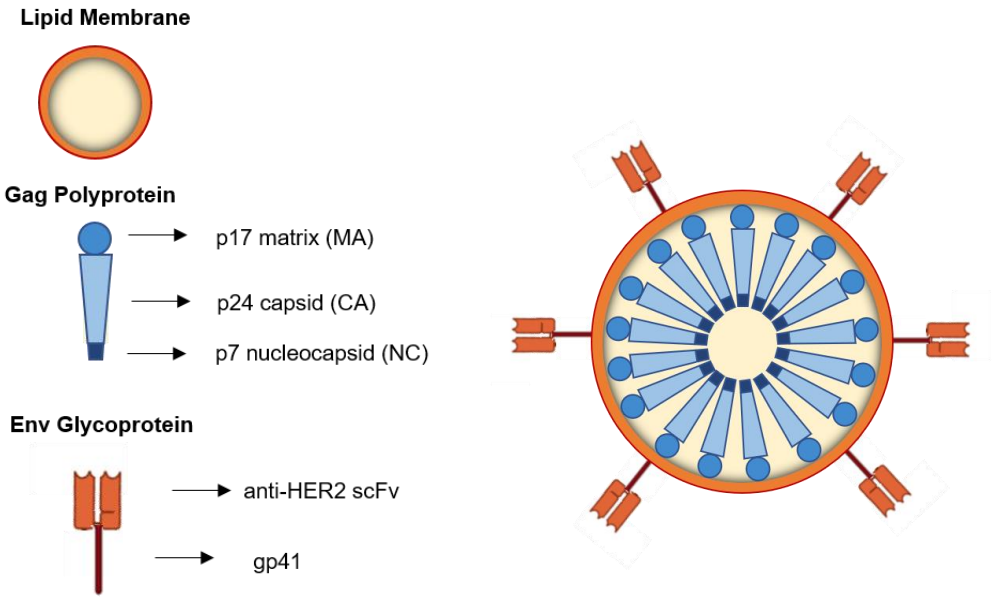

Figure 5: Schematic representation of the HIV-1 based VLP model used in this work.

1.3.1. HIV-1 based VLPs assembly and budding process

Gag is a structural polyprotein constituted by the following major structural proteins: p17 matrix (MA), p24 capsid (CA), p7 nucleocapsid (NC) and p6 linker(LI) protein, and also by small spacer peptides p2 (SP2) and p1 (SP1) (Figure 6) (Deml et al., 2005). This structural polyprotein has the ability to self-assemble into VLPs even in the absence of other viral proteins and viral RNA (Perlman and Resh, 2006; Gutiérrez-Granados *et al.*, 2013; González-Domínguez *et al.*, 2020). This assembly involves cooperative interactions between the multiple domains of the Gag protein. For example, the N-terminal glycine residue from p17 MA (site of myristic acid attachment) is vital for the VLP assembly and the binding of the Gag precursor to the inner leaflet of the plasma membrane (Figure 7) (Deml et al., 2005; Lavado-García et al., 2021). The p17 MA also affects the Env glycoprotein incorporation in the VLP surface. Further studies also suggest the importance of p7 for an efficient targeting and binding of Gag to the cellular membrane (Deml et al., 2005).

The *pol* gene encodes the protease (PR) domain that cleaves Gag into functional subunits. It allows the HIV-1 based VLP lateral movement and the clustering of the Env proteins on the VLP surface (Gonelli et al., 2019).

The envelope HIV gene encodes the gp120 and gp41 (Figure 6). The gp41 is a transmembrane glycoprotein that mediates the membrane fusion and induces viral core entry. The gp120 is an outer layer glycoprotein responsible for viral infection, facilitating the HIV entry into the host cell. It binds to the CD4 receptor and CCR5 and CXCR4 co-receptors of the cell. The gp120 is bound to the gp41 (Figure 7). The HIV Env glycoproteins form hetero-trimers (Garg & Blumenthal, 2008; Yoon et al., 2010, Visciano et al., 2011; Tedbury & Freed, 2014).

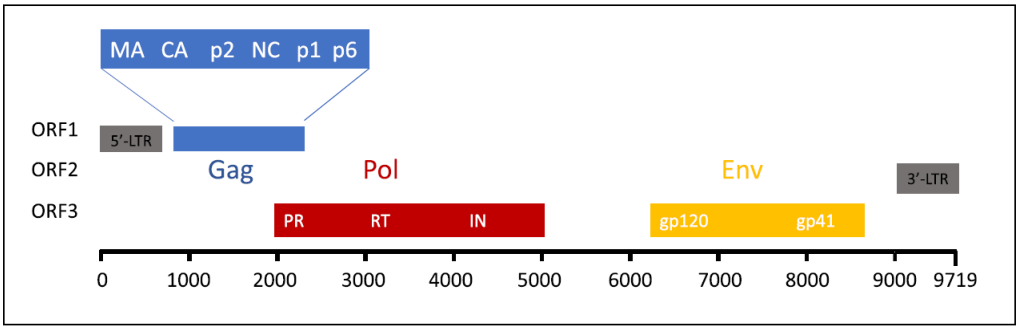

Figure 6: Schematic representation of HIV-1 structural genes (*gag, pol and env*). Adapted from (Cervera et al., 2019).

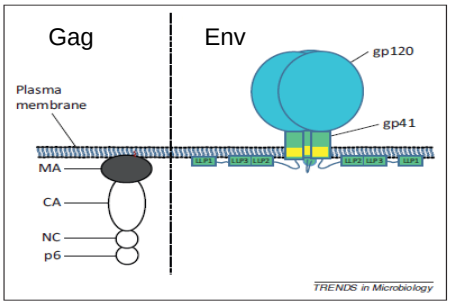

Figure 7: Schematic representation of Gag and Env proteins. Adapted from (Tedbury & Freed, 2014).

The Gag polyproteins are expressed in the cytoplasm of the cell, in cytosolic ribosomes (Deml et al., 2005). These Gag monomers are transported to the cell membrane by the endosomal sorting complex required for transport. These complexes also coordinate the assembly and oligomerization of the Gag monomers that will form protrusion buds in the cell membrane, known as a budding process, and acquire a lipid enveloped from the host cell (Deml et al., 2005; Gutiérrez-Granados et al., 2013; González-Domínguez et al., 2016; Lavado-García, Jorge, et al., 2021). The binding of Gag to the plasma membrane is done through the p17 matrix (MA) domain (Tedbury & Freed, 2014). The buds are later released from the cell membrane to form Gag-VLPs (Figure 8) (Deml et al., 2005; Tedbury & Freed, 2014, Gonelli et al., 2019).

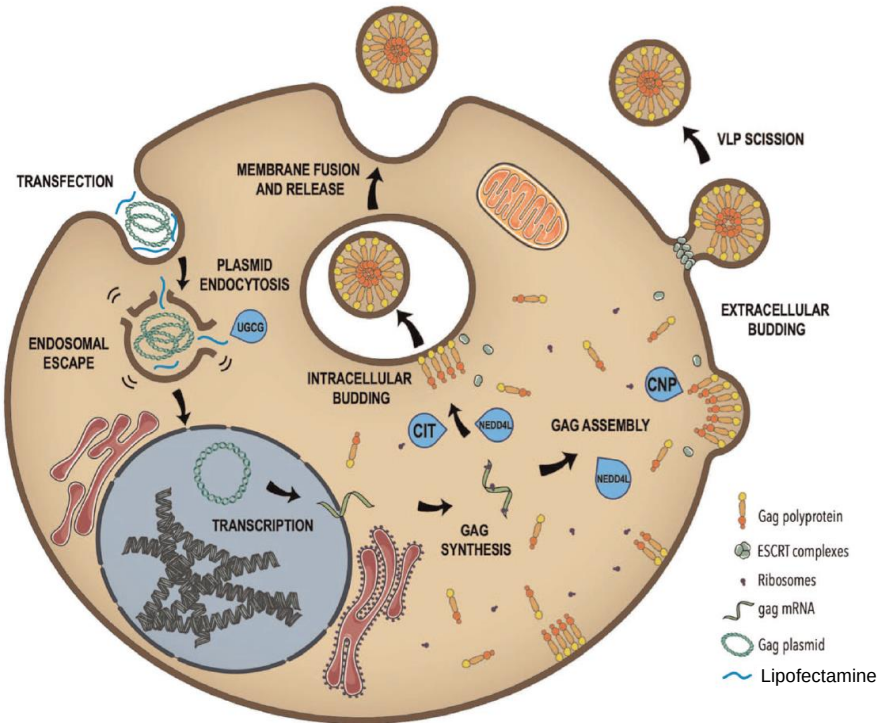

Figure 8: Schematic representation of the VLP production through transient transfection. Adapted from (Lavado-García et al., 2021).

If the host cell expresses not only the *gag*, but also the *env* gene, then Gag-Env VLP will be assembled.

The Env glycoprotein is translated in the endoplasmic reticulum and migrates through the Golgi complex to the plasma membrane (Cervera et al., 2019).

There are four models that explain the incorporation of the Envelope glycoprotein into the Gag-VLPs presented in Figure 9.

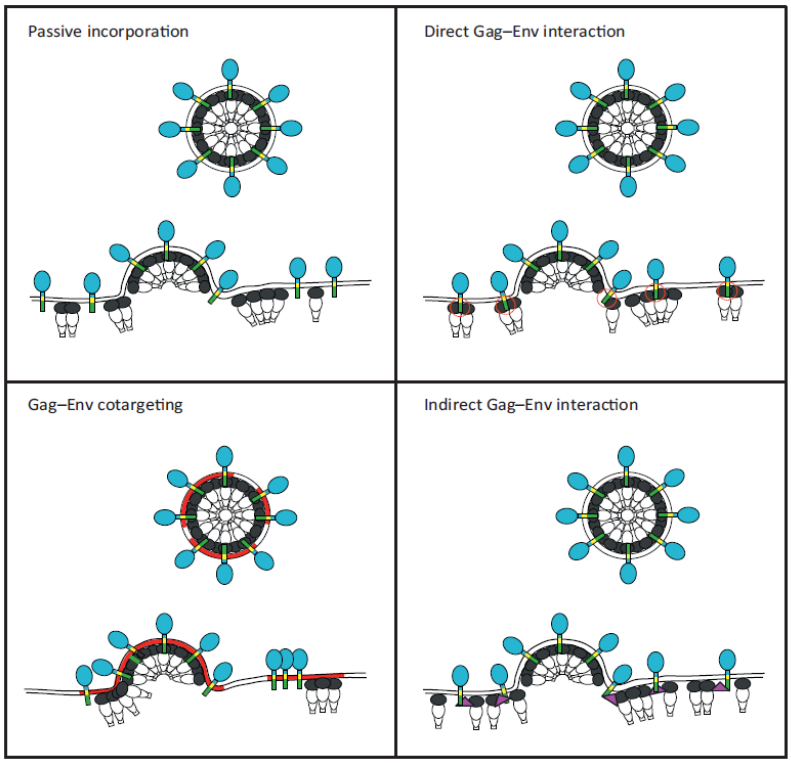

Figure 9: Envelope incorporation models. Gray: MA; blue: gp120; green: gp41; yellow: gp41 transmembrane domain; red: lipid rafts; pink: hypothetical bridging factor. From (Tedbury & Freed, 2014).

The first model is based on a passive mechanism where the Env proteins that are present on the assembly site in the plasma membrane will be incorporated into the VLP surface as the budding is occurring. The second model is related to the co-targeting of Gag and Env, where the Env packaged is enhanced by targeting Gag and Env to lipid rafts in the plasma membrane. The other models involve specific protein-protein interactions, either direct or indirect. The direct Gag-Env interaction model suggests that a direct interaction between the MA of the Gag and the cytoplasmic tail (CT) of the gp41 during particle assembly is necessary for Env incorporation in the VLPs. The indirect Gag-Env interaction model proposes the presence of a cellular factor that binds to Env and Gag, bridging their interaction. This last model suggests that Env incorporation is cell type-dependent (Tedbury & Freed, 2014).

1.3.2. Production in mammalian systems

An HIV-1 based VLP needs a eukaryotic expression system to be produced because it is an enveloped VLP. The mammalian cell system provides the most accurate and complex post-translational modifications vital for the construction of these enveloped VLPs (Chen et al., 2020). The main drawback of this system is the low productivity and the formation of exosomes by the cell that have similar size and properties to the VLPs produced, which makes the downstream process difficult. Nevertheless, this system offers a huge potential in the production of complex enveloped VLPs like the HIV-1 based VLP (Cervera et al., 2019).

The mammalian expression system that has been extensively used to produce these enveloped VLPs is the HEK-293. This cell line is used in both research and industrial environments as it is easy to grow and transfect (Dietmair et al., 2012; Javier Fuenmayor et al., 2018). Moreover, this cell line is able to confer specific post-translational modifications to the VLPs, like N-myristoylation, that are responsible for the correct VLP construction (Lavado-García et al., 2021). The production and optimization of VLPs in these cells have been widely studied. HEK-293 cells after being transiently transfected produced $2.7x10^9$ VLPs/mL (Cervera et al., 2013). An optimization to this protocol was done, where the production period was prolonged by re-transfecting the cell culture and there was exchange of medium with chemical additives (lithium acetate, valproic acid and caffeine). This new method is called extended gene expression (EGE) with additives and produced $4.45x10^{10}$ VLPs/mL. In order to reduce the detrimental effects on the cell growth and viability, the chemical additives were replaced by shRNA encoded in the Gag-GFP plasmid inhibiting HDAC5 and PDE8A, which replaces the valproic acid and caffeine effect, respectively. This new strategy produced $3.88x10^{10}$ VLPs/mL (Javier Fuenmayor et al., 2018).

The CAP-T (CEVEC Pharmaceuticals) cell line is a novelty cell line also used in the production of HIV-1 based VLPs. These cells are capable of growth in a serum-free medium and in suspension, while having high cell densities and expressing recombinant proteins with human post-translational modifications. They can also be transiently transfected with PEI, a transfection reagent. After optimization of the transfection, the CAP-T cells produced $4x10^{10}$ VLPs/mL in a bioreactor. All these characteristics facilitate large-scale transient transfection which is a massive advantage when changing from the development to the production stage (Gutiérrez-Granados et al., 2016, 2017).

An optimized production process of HIV-1 based VLPs must be cost-effective, have high production yields, the possibility to scale-up and also to provide the correct structure and immunogenicity to the VLPs (Cervera et al., 2019).

1.4. Motivation and Aim of the Thesis

According to the World Health Organization, cancer is one of the leading causes of death worldwide. In 2020 nearly 10 million deaths were reported due to cancer, with the most common of those being due to breast cancer [https://www.who.int/news-room/fact-sheets/detail/cancer].

HER2 positive cancer is an extremely aggressive type of cancer, which is associated with a poor prognosis and that can become therapy/drug resistant. It also has a significantly shorter relapse times and overall survival and a higher probability of metastasis (Advani et al., 2015; Dai et al., 2017). From all diagnosed breast cancers, 15%–30% overexpress *HER2*.

In addition, HER2 is a receptor involved in all phases of cell development, becoming an important therapeutic target in the therapy of HER2 positive cancers (Faltus et al., 2004; Yang et al., 2004; Lewis Phillips et al., 2008).

A drug's therapeutic efficacy can be enhanced by increasing its specificity towards its target. Nanoparticles are being studied as targeted therapies due to their recognized ability to improve the packaging, delivery and efficiency of drugs (Gulati et al., 2018). Virus-like particles emerge as promising and exciting nanoplatforms to be used as drug delivery systems due to their biocompatibility and biodegradability (Steinmetz, 2010). To acquire specificity, VLPs need to express a cell-specific target molecule of interest, such as a recombinant protein on the cell's surface. The important advances in biomedical research through the rapid process of recombinant DNA production and protein engineering have been key to the success of these new approaches (Santos et al., 2021). In the case of HER2 positive cancer, an anti-HER2 delivery system is needed to increase the therapeutic index by enhancing the anti-tumour efficacy and reducing the systemic toxicity.

Preliminary work was done where a biomimetic vector containing the scFv of trastuzumab, an anti- HER2 antibody, as a targeting motif fused with HIV-1 viral protein gp41 was designed and produced. Docking studies were performed to select the most favourable residue in the viral protein to be considered to fuse with a scFv from trastuzumab, after which DNA plasmid was produced and validated under the scope of this thesis. This work initially developed allowed for a publication in an international peer-reviewed publication (Santos et al., 2021).

The main objective of this thesis was the development and characterization of an HIV-1 based VLP containing at the surface a scFv of an anti-HER2 antibody. The design of this nanoplatform will allow to obtain a delivery system able to bind to the receptor HER2, and thus deliver therapeutic and/or imaging molecules directly to the cancer cells overexpressing *HER2*.

The specific questions addressed in this thesis are:

1. Is it possible to produce HIV-1 based VLPs?

2. Is the scFv from trastuzumab present at the surface of the HIV-1 based VLP?

3. Does scFv from trastuzumab when expressed on the VLP surface maintains specificity to the HER2?

4. Is the HIV-1 based VLP cytotoxic to the cells?

The overarching goal of the research presented in this thesis is the proof-of-concept of this new approach for targeted therapy using recombinant proteins to be expressed into VLPs that can be designed by *in silico* methods.

This work allowed the publication of a manuscript “Santos, J., Cardoso, M., Moreira, I. S., Gonçalves, J., Correia, J. D. G., Verde, S. C., & Melo, R. (2021). Integrated in Silico and Experimental Approach towards the Design of a Novel Recombinant Protein Containing an Anti-HER2 scFv. International Journal of Molecular Sciences, 22(7). https://doi.org/10.3390/ijms22073547” and inspired the writing and submission of a review manuscript in the scope of HIV-1 based VLPs “Santos J, Silva R, Rosa C, Verde SC, Correia JDG, Melo, R. Natural supramolecular structures from HIV-1 European Journal of Chemical Medicine”.

We will soon compile the remaining experimental results and publish a final manuscript that will serve as a kick-off for future projects aimed at optimising targeted therapies.

2. Materials and Methods

2.1. Bacteria strain and media

NEB® Stable Competent *Escherichia coli* cells (New England Biolabs, Inc.) were grown in TSB medium (30 g TSB in 1 L Milli-Q H_2O) (Oxoid) supplemented with 100 µg/mL of ampicillin (NZYtech, New Zealand) accordingly with the plasmid's selectable marker. The incubations were carried out at 30°C to reduce recombination activity in lentiviral plasmid propagation and cloning. The bacterial strain used for DNA propagation and cloning was transformed following the protocol presented in section 2.3.

2.2. Plasmids

The plasmid DNA (X1665+pcDNA3.1+) containing the anti-HER2 scFv and the viral protein gp41 protein sequence was synthetized in Synbio Tech (NJ, USA). From now on this plasmid DNA will be called pX1665. pMDLg/pRRE, pCMV-VSV and pRSV-REV (Addgene, USA), encode the packaging proteins Gag-Pol, VSV-G and Rev respectively, and were used to produce lentiviral particles for cell internalization. The pMDLg/pRRE includes the *gag* that encodes for the virion main structural proteins, *pol* that is responsible for the retrovirus-specific enzymes and RRE, a binding site for the Rev protein which facilitates export of the RNA from the nucleus. pHR_EGFPligand (Addgene, USA) encodes the EGFP surface ligand. This vector is adapted from the HIV and will integrate its genetic information in the VLP genome.

All plasmid maps are shown in Annexes (Figure A1 – A5).

2.3. Bacterial transformation and selection

Plasmid DNA was added to NEB® Stable Competent *E. coli* and the cells were transformed by electroporation on a Bio-Rad Gene Pulser at 200 Ω, 25 F and 1.8 kV. After the cells were pulsed, LB medium (NZYtech, New Zealand) was added and the cells were incubated at 37ºC with vigorous shaking for 1 h. The transformed cells were plated on a LB-agar plate containing 100 µg/mL of ampicillin (NZYtech, New Zealand) and grown overnight at 37ºC. Then, an isolated colony was picked and grown in 10 mL of LB supplemented with 100 µg/mL of ampicillin at 37ºC with agitation. After 16 h, the cell culture was centrifuged for 10 min at 3095 rpm (Beckman, J2-21M, Beckman Coulter, Inc., USA) at room temperature, resuspended in LB medium with 10% (v/v) of glycerol and stored at -80ºC.

2.4. DNA extraction and quantification

DNA was extracted and purified using the GF-1 Bacterial DNA Extraction kit (Vivantis, Malaysia), according to the manufacturer's instructions taking into consideration that the cells are Gram negative. Then, the DNA concentration and purity were determined using the Varioskan™ LUX (ThermoFisher Scientific®, MA, USA).

2.5. Cell culture

HEK-293T cells (human embryonic kidney-293 cells expressing the large T-antigen of simian virus 40), SK-BR-3 (human breast adenocarcinoma cell line HER2-positive) and MDA-MB-231 (human breast adenocarcinoma cell line HER2-negative) were grown in DMEM (Dulbecco's modified Eagle's medium) supplemented with 6 mM L-glutamine, 1 nM sodium pyruvate, 0.1 nM MEM Non-Essential Amino Acids, 10% (v/v) fetal bovine serum and 1% (v/v) penicillin-streptomycin, all obtained from Cytiva (USA). HEK-293T cells were cultured in a static system using disposable polycarbonate 75 cm^3 flasks at 37°C with 5% of CO_2, while SK-BR-3 and MDA-MB-231 cells were cultured in disposable polycarbonate 25 cm^3 flasks in the same conditions as previously mentioned. All cell lines were tested for mycoplasma using the LookOut® mycoplasma PCR Detection Kit.

Cell concentration and viability were assessed by haemocytometer cell counts using trypan blue exclusion dye (Merck, Germany).

2.6. Transfection

A transfection method can be used to introduce artificially nucleic acids into cells, which can confer to the transfected cells the ability to produce VLPs. The transfection method chosen was chemical since we have access to easy and fast protocols with high efficiency and expression performance (Maurisse et al., 2010; Shi et al., 2018). A cationic lipid-based reagent will coat the negatively charged DNA, and allow its introduction into the negatively charged cell membrane (Gharagozloo et al., 2015).

In this work, Invitrogen™ Lipofectamine™ 3000 was used to perform the transient transfection method shown in Figure 10.

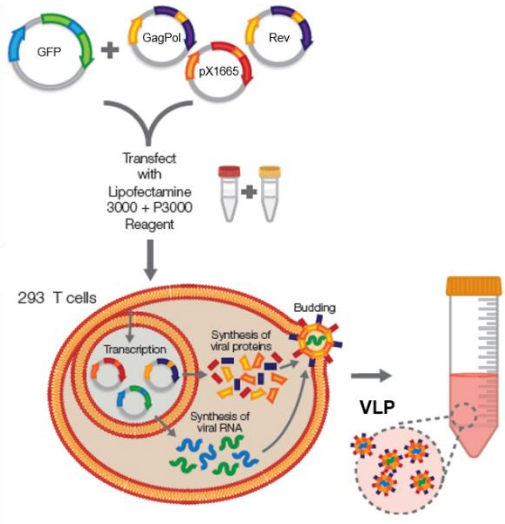

Figure 10: Schematic representation of the transfection protocol. Adapted from ThermoFisher Application Note from Lipofectamine 3000 Transfection Reagent.

The plasmid DNA is complexed with lipid reagents to mediate an efficient delivery into the cell's nucleus. This reagent shows the highest transfection efficacy in HEK-293 cells (Shi et al., 2018; T. Wang et al., 2018). However, the association of Lipofectamine 3000 with P3000 increases the cytotoxicity to the cells compared to other reagents (T. Wang et al., 2018). This fact can be overlooked because a transient transfection is a fast process, where the DNA of interest is not integrated in the genome of the transfected cells (Kim & Eberwine, 2010; Javier Fuenmayor et al., 2018). So, the most important factor with this type of transfection is the high titres of VLPs that can be obtained by this reagent and not the cell viability after the transfection protocol. In conclusion, Lipofectamine™ 3000 is a highly efficient, simple, fast, easy to use and cost-effective product for lentiviral production that also allows large gene sizes.

In this work eleven batches were produced with different transfection conditions, differing in the cell density, plasmids used and ratios of plasmids. The protocols of each batch are presented below.

2.6.1. HIV-1 based VLP production

For batch 1, HEK-293T cells were seeded on uncoated 10 cm plates at a density of 7.0×10^6 cells/plate and incubated overnight at 37ºC and 5% CO_2. Lipofectamine™ 3000 (ThermoFisher Scientific®, MA, USA) was used to transfect the cells with 17.5 µg of pX1665 and 21.0 µg of pMDLg/pRRE. Subsequently, the cells were incubated for 6 h at 37ºC and then the medium was replaced with fresh medium. At 24 h post-transfection, the supernatant was collected and replaced with 12 mL of fresh cultured medium, and at 52 h the supernatant was collected again. Both collections were combined and centrifuged at 2000 rpm (Beckman, J2-21M, Beckman Coulter, Inc., USA) at room

temperature for 10 min. The supernatant containing the VLPs produced was collected and stored at - 80ºC for later use. The experimental protocol is described in Figure 11.

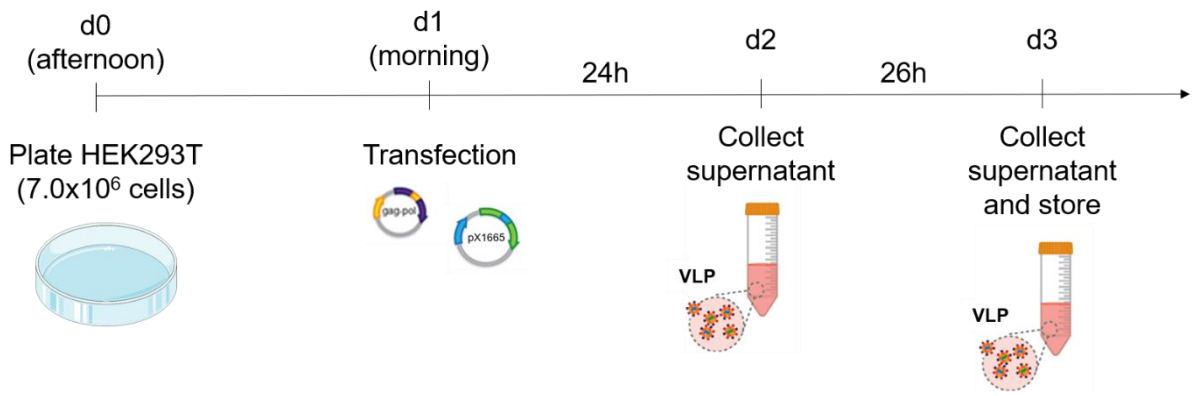

Figure 11: Experimental protocol for HIV-1 based VLP production.

2.6.2. Production optimization

For batch 2 and 3, the transfection was optimized and a density of 6.0x10^6 cells/plate was used. Lipofectamine™ 3000 (ThermoFisher Scientific®, MA, USA) was used to transfect the cells with 17.5 µg of pX1665, pMDLg/pRRE and pRSV-REV. The experimental protocol and optimizations performed are described in Figure 12.

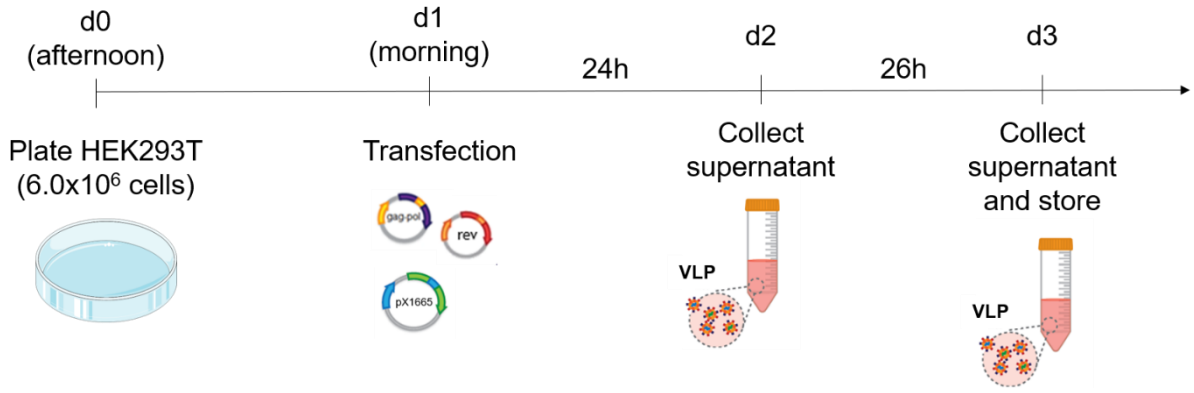

Figure 12: Experimental protocol for the optimization of the HIV-1 based VLP production.

2.6.3. Expression of scFv anti-HER2+gp41 fusion protein

HEK-293T cells were seeded on 6-well plates at a density of $0.5x10^6$ cells/well. Lipofectamine™ 3000 (ThermoFisher Scientific®, MA, USA) was used to transfect the cells with 2.5 µg of pX1665. At 24 h post-transfection, the medium was replaced with 2 mL of fresh medium supplemented with 500 µg/mL of kanamycin (NZYtech, New Zealand) accordingly with the plasmid's selectable marker. At 52 h post-transfection the cells were recovered. The experimental protocol performed is described in Figure 13.

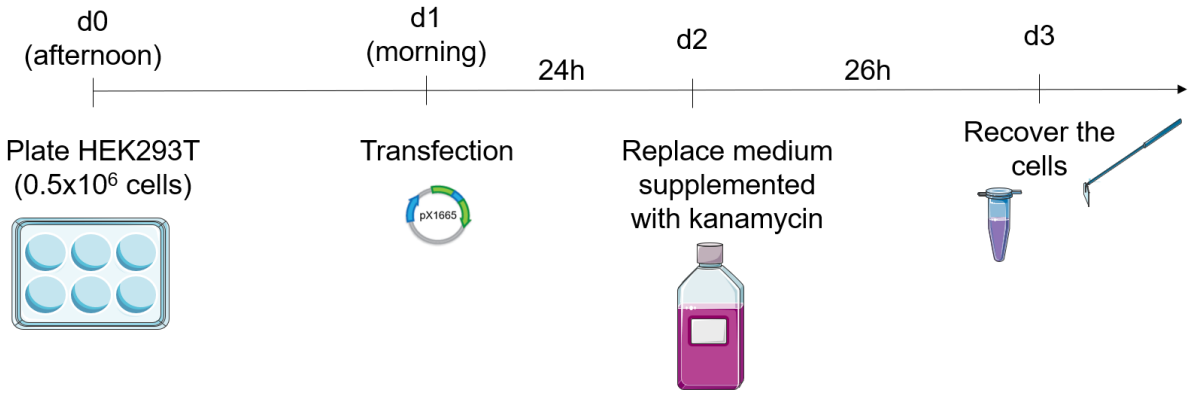

Figure 13: Experimental protocol to evaluate the design plasmid.

2.6.4. Evaluation of different ratios of pX1665

HEK-293T cells were seeded on 6-well plates at a density of $1.0x10^6$ cells/well. Lipofectamine™ 3000 (ThermoFisher Scientific®, MA, USA) was used to transfect the cells with the masses presented in Table 2. The supernatant was collected 48 h post-transfection.

Table 2: DNA quantities used for HEK-293T cells transfection taking into account the size of the plasmid (Annexes Figure A1-A3). Ratios are presented as number of plasmid as pX1655: pMDLg/pRRE: pRSV-REV.

	pX1655: pMDLg/pRRE: pRSV-REV	Mass (µg)		
	ratio	pX1665	pMDLg/pRRE	pRSV-REV
Batch 4	1:1:1	1.02	1.35	0.63
Batch 5	2:1:1	1.52	1.01	0.47
Batch 6	5:1:1	2.16	0.57	0.27
Batch 7	10:1:1	2.51	0.33	0.16

The experimental protocol is described in Figure 14.

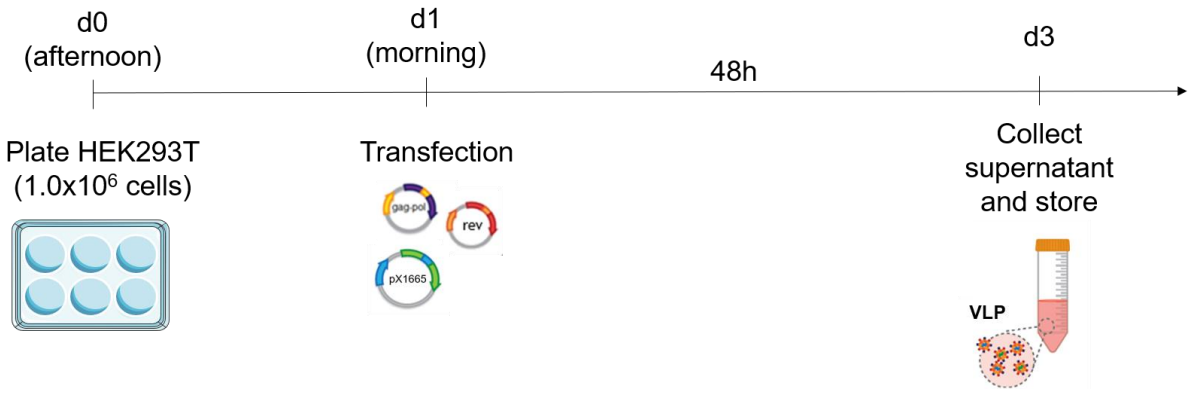

Figure 14: Experimental protocol to produce HIV-1 based VLPs using different ratios of the plasmid pX1665.

2.6.5. HIV-1 based VLP production for binding assay

Lipofectamine™ 3000 (ThermoFisher Scientific®, MA, USA) was used to transfect the cells with the masses presented in Table 3.

Table 3: DNA quantities used for HEK-293T cells transfection taking into account the size of the plasmid (Annexes Figure A1-A5). For the different batches, ratios are presented as pX1655: pMDLg/pRRE: pRSV-REV: pHR_EGFPligand.

	pX1655: pMDLg/pRRE: pRSV-REV: pHR_EGFPligand ratio	**Mass (µg)**				
		pX1665	pMDLg/pRRE	pRSV-REV	pCMV-VSV-G	pHR_EGFPligand
Batch 8 and 10	1:1:1:1	0.67	0.90	0.42	-	1.01
Batch 9 and 11	5:1:1:1	1.76	0.47	0.22	-	0.53
Positive Control	n/a	-	0.90	0.42	0.66	1.01

The experimental protocol is described in Figure 15.

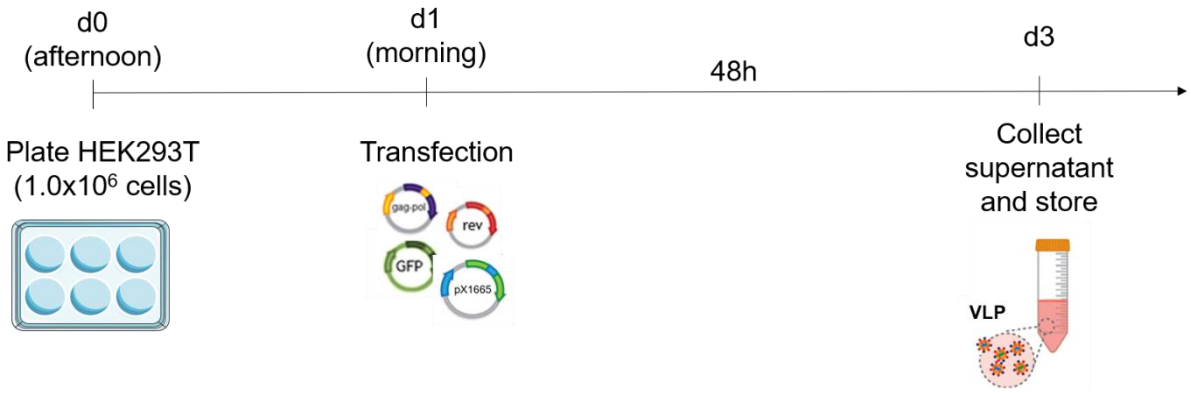

Figure 15: Experimental protocol to produce HIV-1 based VLPs for posterior incubation and analyse.

2.7. Total protein extraction and quantification

After the cells were recovered in section 2.6.3, a lysis buffer (Roche, Switzerland) supplemented with protease inhibitors (Roche, Switzerland) was added and the cells were incubated at 4ºC with agitation for 15 min. Then, the cells were centrifuged at 13249 rpm (Beckman, J2-21M, Beckman Coulter, Inc., USA) during 15 min and the cell extract was collected. Total protein quantification of the cell extracts was determined using the DC Protein Assay (BioRad, USA) according to the manufacturer's instructions. For the calibration curve, bovine serum albumin (BSA) standard solutions were used in the range of 0-10 mg/mL. The absorbance at 750 nm was measured on a PowerWase™ XS Microplate reader (BioTek, USA).

2.8. VLP quantification - ELISA

The structural protein that constitutes the capsid of the HIV-1 based VLPs is p24 (J Fuenmayor et al., 2017: Fink & Campbell, 2018; Cervera et al., 2019).

Quantification of the HIV-1 based VLPs was done using the INNOTEST HIV Antigen mAb (Fujirebio, Japan). This ELISA method allows the detection and quantification of any HIV based lentiviral supernatant. The microtiter plate wells are coated with biotinylated anti-p24 monoclonal antibodies, which will bind to the HIV-1 p24 present in the test samples. The absorbance at 450 nm was measured on an EZ Read 800 Microplate Reader (Biochrom, USA) and quantified against a p24 standard curve.

2.9. Western blot

Expressed proteins in the cell extracts and supernatants were visualized by Western blotting. Samples and positive control (protein extract containing HA) were mixed with 1/6 of 6X SDS sample buffer and boiled for 10 min at 95°C. Then, they were loaded per well and migrated on a 12.5% SDS-PAGE gel. After electrophoresis, the samples were transferred to a nitrocellulose membrane (BioRad, USA). The membranes were blocked at room temperature for 45 min with 5% (w/v) non-fat dried milk in PBS buffer containing 0.2% (v/v) Tween 20. Then, different antibodies were used for each membrane. One membrane was incubated for 90 min at room temperature with gentle agitation with HRP (horseradish peroxidase)-conjugated anti-HA polyclonal antibody (Fisher Scientific, USA) diluted 1:2500 or 1:10000 in 1% (w/v) non-fat dried milk in PBS buffer containing 0.2% (v/v) Tween 20. While other membranes were incubated for 60 min with the primary antibodies presented in Table 4. After washing with PBS Tween 0.2% (v/v), these last membranes were incubated with the secondary antibody anti-mouse (BioRad, USA) diluted 1:3000 in 1% (w/v) non-fat dried milk in PBS buffer containing 0.2% (v/v) Tween 20 for 60 min at room temperature. Then all membranes were washed with PBS Tween

0.2% (v/v) and the proteins were visualized using the ECL® reagent (GE Lifesciences, USA) according to the manufacturer's instructions.

Table 4: Primary antibodies used for Western blotting.

Antigen	Company	Host	Clonality	Dilution
HA (901502)	Biolegend	Mouse	monoclonal	1:2000
HA (SC-57592)	Santa Cruz Biotechnology, Inc	Mouse	monoclonal	1:200
HA (SC-7392)	Santa Cruz Biotechnology, Inc	Mouse	monoclonal	1:200

2.10. Cell incubation with HIV-1 based VLPs for binding assay

The supernatant collected after the transfection containing the HIV-1 based VLPs was added to HER2 positive cells, the SK-BR-3, and HER-2 negative cells, the MDA-MB-231.

$7.5x10^4$ SK-BR-3 cells and $5.0x10^4$ MDA-MB-231 cells were plated in 24-well plates and incubated at 37ºC for 48 h. Then, different dilutions (1/2, 1/5 and 1/10) of the VLPs produced in section 2.6.5 were added to the cells. After 24 h of incubation at 37ºC, the cells were analysed by flow cytometry.

2.11. Flow cytometry

Cells were collected from the 24-well plate with EDTA (10mM) in PBS and centrifuged at 1623 rpm (Beckman, J2-21M, Beckman Coulter, Inc., USA) for 5 min. After, cells were re-suspended in 200 µL of PBS 1% BSA + EDTA (1mM) and collected. These samples were analysed in Cytek™ Aurora system (Cytek Biosciences, Inc, USA) to evaluate the binding specificity of these cells to the VLPs produced, by measuring the green fluorescent intensity present in the incubated cells. This system is equipped with 4 lasers (violet-405nm, blue-488nm, green/yellow-561nm, red-640nm), forward and side scatter detectors and 64 fluorescent emission detectors. The equipment was calibrated using the 2003 Beads following the manufacturer's instructions. Analysis from 10000 events per sample was done using FlowJo software (FlowJo, LLC).

2.12. Cytotoxicity assay - WST-1 proliferation test

Cell viability was evaluated using the WST-1 proliferation test. SK-BR-3 cells were seeded in 96-well plate at a density of $1.0x10^5$ cells/well and incubated at 37ºC for 52 h. Different dilutions (1/2, 1/5 and 1/10) of the VLPs produced in section 2.6.5 were added to the cells. After 24 h of incubation at 37ºC, the inoculum from the wells was removed and replaced with 100 µL of fresh medium (DMEM 10% FBS) and 10 µL of a cell proliferation reagent WST-1 (Roche, Switzerland). After gentle mixing, the cells were incubated at 37ºC for 6 h. The absorbance was measured on an EZ Read 800 Microplate Reader (Biochrom, USA) at 450/620 nm.

3. Results and Discussion

The main purpose of this thesis was the development and characterization of an HIV-1 based VLP that contains at the surface a scFv of an anti-HER2 antibody. The work can be divided in the: 1) HIV-1 based VLP production and quantification, 2) evaluation of the scFv from trastuzumab in the VLP, 3) assessment of VLP-HER2 binding and 4) evaluation of the cytotoxic effect of the VLP.

3.1. HIV-1 based VLP production and quantification

Virus-like particles, such as HIV-1 based VLPs, are produced upon heterologous expression in a host system. The capsid proteins self-assemble and form VLPs, which can be purified from the cells or the cell culture supernatant, depending on the expression system chosen (see section 2.6.).

HIV-1 based VLP is an enveloped VLP, which means that it needs a eukaryotic expression system to be produced (Chen et al., 2020). The mammalian HEK-293T cells were chosen to produce the HIV- 1 based VLPs because they provide the proper protein folding and post-translational modifications required for its function (Cervera et al., 2013, 2019; Zeltins, 2013; Lua et al., 2014; J Fuenmayor et al., 2017; González-Domínguez et al., 2020; Nooraei et al, 2021).

Batch 1 followed the transfection protocol presented in section 2.6.1.

The expression of the Gag protein was determined by ELISA (p24 protein quantification) to evaluate the total concentration of HIV-1 based VLPs.

Serial dilutions of standard solutions were analyzed by p24 ELISA at 450 nm (Figure 16).

A quadratic regression between absorbance at 450 nm and p24 concentration values was observed with an R^2 of 0.9997.

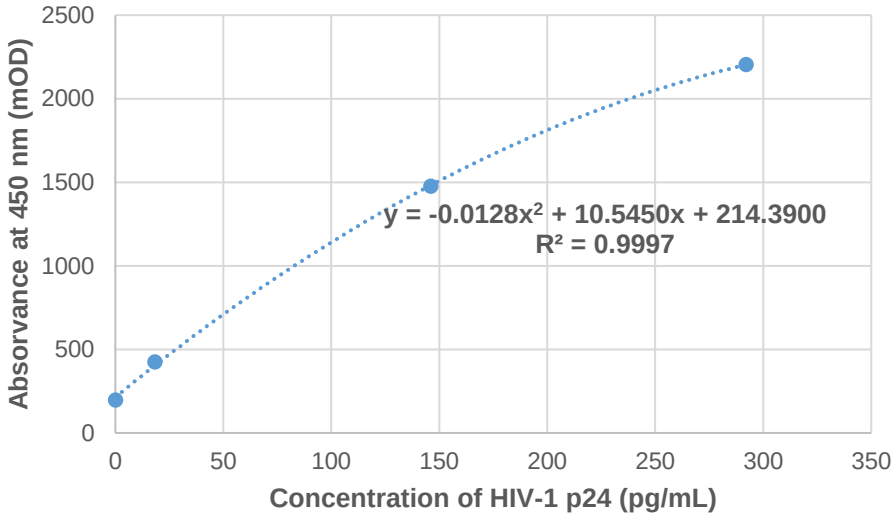

Figure 16: INNOTEST™ HIV Antigen mAb Standard Curve. The dotted line corresponds to the quadratic regression of the absorbance versus the sample concentration.

The correlation equation for HIV-1 based VLPs is as follows:

$$y = -0.0128x^2 + 10.5450x + 214.3900 \quad \textbf{(1)}$$

Equation (1) can be used to calculate pg/mL of p24 (x) of the unknown sample through the absorbances (y). The p24 concentration of batch 1 is 3.88 pg/mL

The VLP concentration obtained with the protocol presented in section 2.6.1 was unexpectedly low (3.88 pg/mL) when compared to the concentrations found in the literature. Gonelli was able to produce 3.62 ng/mL to 33.8 ng/mL Gag-Env VLPs when the *env* gene was also transfected (Gonelli et al., 2019) and other studies when only the *gag* was transfected were able to produce up to 2.8 µg/mL Gag-VLPs (Cervera et al., 2013, 2019; González-Domínguez et al., 2020). An optimization of the transfection protocol was performed to overcome this issue.

3.2. HIV-1 based VLP production optimization and quantification

As previously mentioned, the Gag polyprotein expressed by the *gag* gene self-assembles and forms the HIV-1 based VLP (Cervera et al., 2019; González-Domínguez et al., 2020). The transcription of HIV structural genes, such as *gag* and *pol*, is modulated by *rev*, a regulatory gene (Cervera et al., 2019).

The 3rd Generation Lentiviral System uses a packaging system split into two plasmids: one encoding *rev* (pRSV-REV) and one encoding *gag* and *pol* (pMDLg/pRRE) improving the process yields (Dull et al., 1998). For these reasons, the pRSV-REV was added to cells together with the other plasmids. Additionally, an optimization of the number of cells plated was also done. Where cell density was decrease because transfection efficiency decreases substantially at higher cell densities (Cervera et al., 2019).

Batch 2 and 3 followed the transfection protocol presented in section 2.6.2. The p24 concentration of batch 2 and 3 was calculated as in section 3.1. with equation (2) and (3), respectively.

$$y = 0.0002x^2 + 8.2418x + 140.6100 \quad \textbf{(2)}$$

R^2=0.9982

$$y = -0.0091x^2 + 10.8880x + 117{,}7000 \quad \textbf{(3)}$$

R^2=0.9999

Batch 2 and Batch 3 have a concentration of p24 of 193.56 ng/mL and 33.64 ng/mL, respectively.

The VLP concentrations obtained with the protocol presented in section 2.6.2. were similar to the ones found in the literature as cited previously (Cervera et al., 2013, 2019; Gonelli et al., 2019; González-Domínguez et al., 2020).

Comparing the results obtained by the transfection protocol optimization and the previous transfection protocol it suggests that the addition of the *rev* plasmid (pRSV-REV) and the decrease of the number of cells when plating the HEK-293T cells improved the production of the VLPs. The transfection method is an extremely demanding process to the cells (Lavado-García et al., 2020), affecting the cell viability. Decreasing the number of cells promoted the healthy growth of the cells taking into account the specific area of the plate. These results suggest that a higher number of cells does not imply a higher titre of VLPs produced as previously referred (Cervera et al., 2019).

Despite the fact that batches 2 and 3 were produced using the same protocol, the difference in the concentration obtained is significantly high, seeing that the concentration of batch 2 is almost 6 times higher than batch 3.

The success of the transfection depends on different factors, such as cells, media, the molecule being transfected, and ratios of plasmids, but one of the most important aspects for the efficient

production of VLPs is the condition of the transfected cells. The main difference between batch 2 and batch 3 is the passage and holding status of the HEK-293T cells at the time of transfection. During the batch 2 assay, HEK-293T cells were at passage 23 and, 6 h post-transfection there were about 25% non-adherent cells. Meanwhile, in the batch 3 experiment the HEK-293T cells were at passage 27 and before transfection the cells were already approximately 30% non-adherent and 6 h post-transfection they were about 60%. In both cases, it was also observed that after the first recovery of the supernatant and medium replacement, some cells were no longer adherent, even when collection was done with extreme caution.

When comparing the results obtained between the two batches and what occurs in each individual experiment, it can be concluded that the state of conservation of the cells is a limiting factor in the efficiency of VLP production. Another aspect that can affect the production of VLP is the passage in which the cells were. Further studies were done later regarding the effect of the passage in the transfection efficiency.

3.3. Presence of trastuzumab scFv on the HIV-1 based VLP

The constructed DNA plasmid encoding the scFv-HER2_gp41 sequence, previously done, has a tag for protein detection, N-terminal HA-tag (Annexes_Figure A1). The presence of this fusion protein in the produced VLPs is assessed through a Western blot protocol.

Figure 17: Western blot analysis. 1: batch 2; 2: batch 2 diluted 1/10; 3: batch 3; 4: batch 3 diluted 1/10, 5: positive control (protein extract containing HA). Western blot detection was performed using a Fisher Scientific HRP-conjugated anti-HA polyclonal antibody (1:2500). Visualization of bands was carried out using the ECL® reagent.

In the Western blot result (Figure 17) only the positive control sample (protein extract containing HA) appears to have the HA tag present. This result suggests that the VLPs produced in batches 2 and 3 do not contain the fusion protein (scFv-HER2_gp41). This can be due to a problem in the construction

of the VLP, where budding is not occurring between the gag and the fusion protein. This error may occur due to 1) the fact that the fusion protein is not present around the cell membrane when the budding process occurs, or 2) a problem in the construction of the plasmid DNA, making it impossible to express the fusion protein. Further studies were done to understand the reason for the lack of HA tag in the VLP.

3.4. Plasmid expression and total protein quantification

To assess the quality of the pX1665 plasmid construct, HEK-293T cells were transiently transfected with the X1665 vector, as presented in section 2.6.3. In addition, and to confirm whether it is due to the plasmid that the fusion protein is not expressed in VLP, we performed a further bacterial transformation and DNA extraction as described in section 2.3 and 2.4. After 52 h post-transfection, the cells were collected and lysed to assess through the Western blot technique the expression of the plasmid in this cell line. The plasmid validation was published in an international peer-reviewed publication (Santos et al., 2021).

Total protein of the cell extract was quantified following the protocol presented in section 2.7. The absorbances values at 750 nm of the BSA standard solutions were plotted against BSA concentrations (Figure 18). The values were fitted to a linear regression with an R^2 of 0.9884.

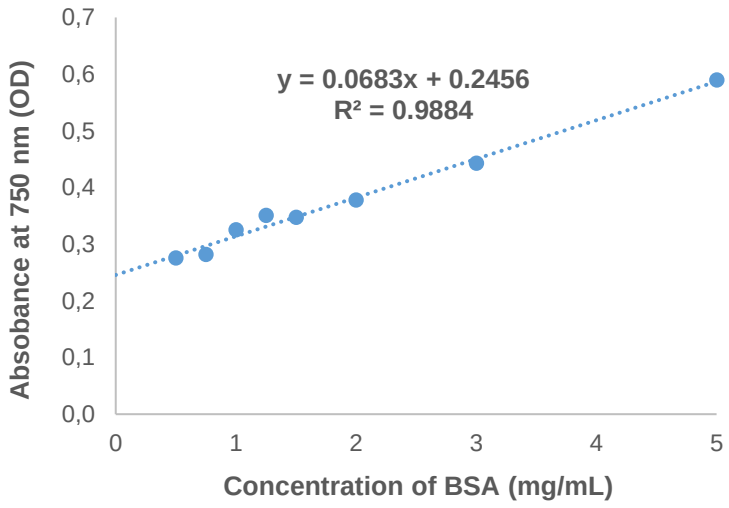

Figure 18: BioRad™ DC Protein Assay Standard Curve. The dotted line corresponds to the linear regression of the absorbance versus the sample concentration.

The concentration of the total protein cell extract (x) of the unknown samples was calculated through the absorbances (y) of the respective samples by applying Equation (4).

$$y = 0.0683x + 0.2456 \quad \textbf{(4)}$$

The results are presented in Table 5.

Table 5: Total protein cell extract concentration. Kan^- : medium added without kanamycin. Kan^+ : medium added with kanamycin. pX1665 (2016): sample that followed the transfection with the plasmid pX1665 extracted in 2016 and stored at -20ºC. pX1665 (2020): sample that followed the transfection with the plasmid pX1665 extracted in 2020 and stored at - 20ºC.

	[Total Protein from Cell Extract] (µg/µL)
HEK-293T Kan^-	3.94
HEK-293T Kan^+	2.80
pX1665 (2016) Kan^+	0.95
pX1665 (2020) Kan^+	0.75

Next, we performed an immunoblot analysis using an anti-HA antibody and the presence of scFv-HER2_gp41 expressed intracellularly in HEK-293T cells was observed (Figure 19).

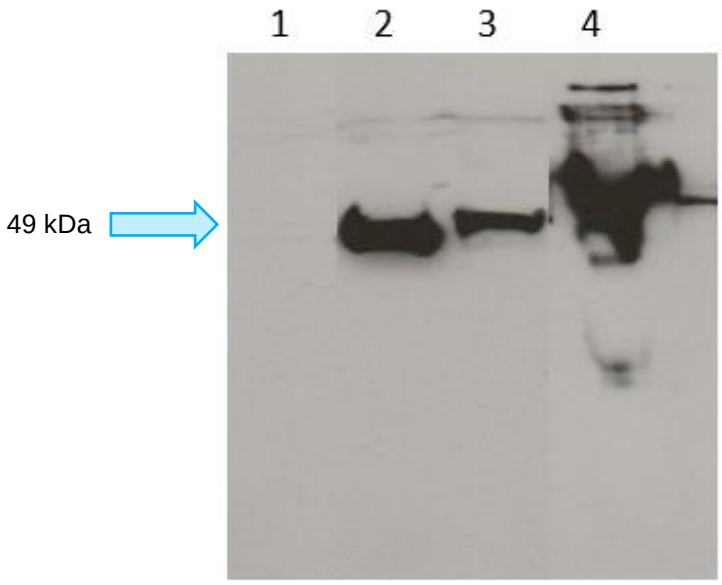

Figure 19: Western blot analysis. 1: negative control (transfection without a plasmid); 2: scFv-HER2_gp41 protein (transfection with plasmid X1665 from 2016); 3: scFv-HER2_gp41 protein (transfection with plasmid X1665 from 2020); 4: positive control (protein extract containing HA). Western blot detection was performed using a Fisher Scientific HRP-conjugated anti-HA polyclonal antibody (1:2500). Visualization of bands was carried out using the ECL® reagent.

The expected molecular weight of the recombinant protein is 47.1 kDa. The molecular weight of the protein expressed by the cells is about 49 kDa (Figure 19, 3 and 4), slightly higher than the theoretical value. Looking at Figure 19, well 2 and 3, we can confirm the presence of the scFv-HER2_gp41 protein in the cell extract (Santos et al., 2021). Also, it shows (Figure 19, well 2 and 3) that both plasmids (plasmid X1665 from 2016 and 2020, respectively) are able to be expressed inside the HEK-293T cells, therefore the plasmid can be stored at -20ºC for a long period and still maintain its viability.

3.5. Optimization transfection with different ratios of x1655 and quantification

Once the quality of the constructed plasmid was confirmed (section 3.4), we went to check for other possible problems and developed a new transfection protocol. The potential problems could be due to the fact that the fusion protein, after being expressed, is not close to the cell membrane, not allowing the budding between the Gag and the fusion protein, or the low amount of pX1665 plasmid, which will not express the fusion protein in a significant quantity, which will not allow the budding and correct VLP construction.

This new transfection protocol takes into account not only different ratios of the plasmid pX1665, but also a single generation of the VLPs (48 h post-transfection). This change takes into account the results of section 3.2., where we concluded that collection of the first generation of VLPs disrupted the cells and decreased their viability leading to a decrease in VLP production.

Batches 4 to 7 followed the transfection protocol presented in section 2.6.4.

The p24 concentration of batches 4 to 7 was calculated as in section 3.1., with equation (5), and the total protein concentration of the cell extracts as in section 3.4., applying equation (6). The results are presented in Table 6.

$$y = -0.010x^2 + 8.942x + 136.290 \quad \textbf{(5)}$$

R^2=0.9922

$$y = 0.0803x + 0.2698 \quad \textbf{(6)}$$

R^2=0.953

Table 6: p24 concentration of the HIV-1 based VLPs produced by the protocol presented in section 2.6.4. and the respective total protein concentration of the cell extracts.

Batches	**pX1655: pMDLg/pRRE: pRSV-REV ratio**	**[p24] (ng/mL)**	**[Total Protein from Cell Extract] (µg/µL)**
4	1:1:1	1.41	8.56
5	2:1:1	1.24	4.91
6	5:1:1	0.81	6.75
7	10:1:1	1.26	7.64

The results presented in Table 6 show that different ratios of the pX1665 do not affect the production of HIV-1 based VLPs.

3.6. Western blot: anti-HA antibody selection

Several antibodies were studied to select the best one, since the western blot results (data not shown) presented a lack of specificity with the new commercially available HRP-conjugated anti-HA polyclonal antibody (Figure 20).

Four antibodies were tested (Table 4 section 2.9) and the corresponding western blot results are presented in Figure 20 and Figure 21. The primary antibody from Biolegend was selected because, as can be seen in Figure 21, it is the one that presents better specificity.

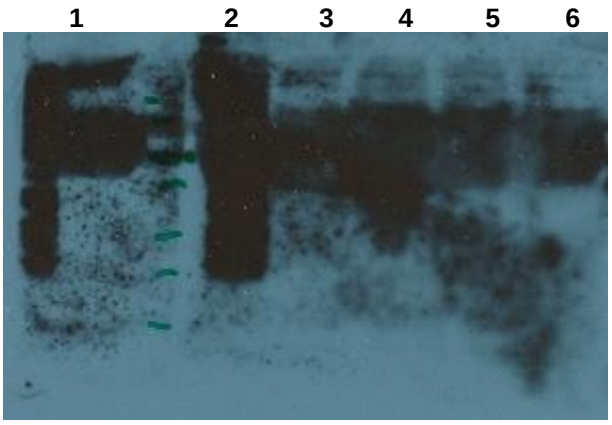

Figure 20: Western blot analysis. 1: batch 2; 2: batch 4; 3: batch 5; 4: batch 6; 5: batch 7; 6: positive control (protein extract containing HA). Western blot detection was performed using a Fisher Scientific HRP-conjugated anti-HA polyclonal antibody (1:2500). Visualization of bands was carried out using the ECL® reagent.

None of the samples and positive controls appeared in the western blots performed with the two antibodies from Santa Cruz Biotechnology, Inc.

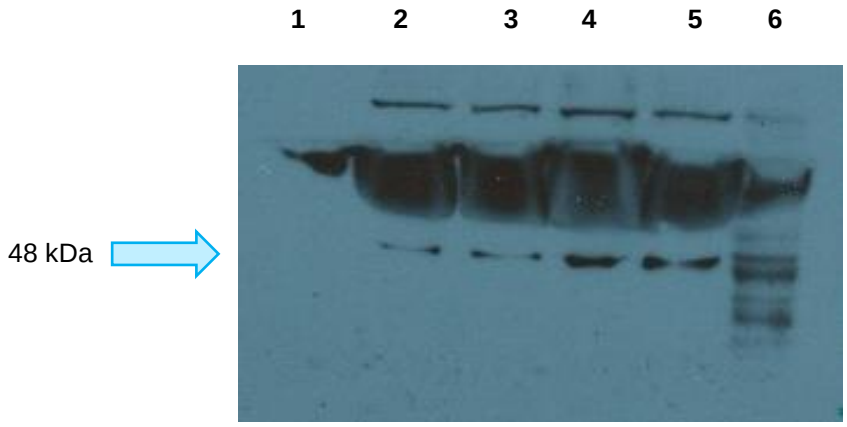

Figure 21: Western blot analysis. 1: batch 2; 2: batch 4; 3: batch 5; 4: batch 6; 5: batch 7; 6: positive control (protein extract containing HA). Western blot detection was performed using a Biolegend primary monoclonal anti-HA-antibody (1:2000) and a BioRad secondary antibody anti-mouse (1:3000). Visualization of bands was carried out using the ECL® reagent.

3.7. Presence of trastuzumab scFv on the HIV-1 based VLP

In order to assess whether assembly of the Gag VLP with the scFv-HER2_gp41 fusion protein was successful, we ran a Western blot protocol with the supernatant (Figure 22) and cell extracts samples (data not shown).

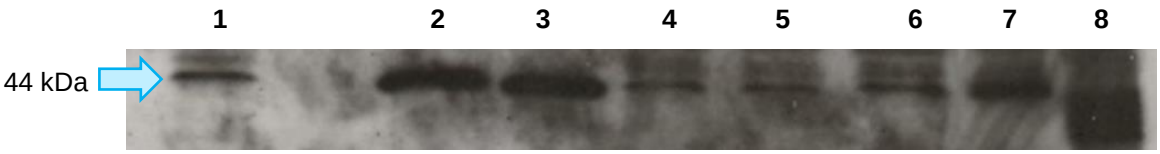

Figure 22: Western blot analysis. 1: negative control (transfection without a plasmid); 2: batch 2; 3: batch 3; 4: batch 4; 5: batch 5; 6: batch 6; 7: batch 7; 8: positive control (protein extract containing HA). Western blot detection was performed using a Biolegend primary monoclonal anti-HA-antibody (1:2000) and a BioRad secondary antibody anti-mouse (1:3000). Visualization of bands was carried out using the ECL® reagent.

Figure 22 shows the immunoblot analysis with an anti-HA antibody. The molecular weight of the protein expressed by the cells is about 44 kDa (Figure 22), slightly lower than the theoretical value. These results confirm the presence of scFv-HER2_gp41 protein in the supernatant pointing to the successful construction of VLP expressing scFv-HER2_gp41protein.

In Figure 22, in well 1 (negative control) a small band appears looking like protein leakage from adjacent wells. To confirm this phenomenon, a new western blot was performed (Figure 23), where the samples were interspersed by an empty well.

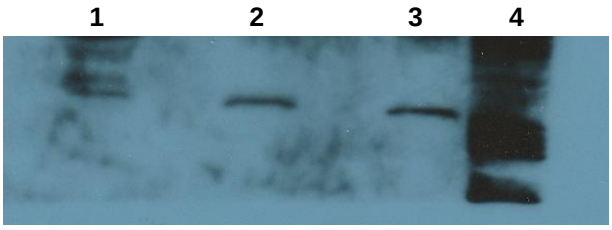

Figure 23: Western blot analysis. 1: negative control; 2: batch 2; 3: batch 3; 4: positive control (protein extract containing HA). Western blot detection was performed using a Biolegend primary monoclonal anti HA-antibody (1:2000) and a BioRad secondary antibody anti-mouse (1:3000). Visualization of bands was carried out using the ECL® reagent.

As can be observed in Figure 23, the pattern of the negative control in the Western blot in the molecular weight range of the VLP is not the same as in the sample bands of batch 2 and 3 (Figure 23, well 2 and 3). However, when compared to batches 4 to 7, well 4 to 7 in Figure 22, respectively, the same pattern appears. Batches 4 to 7 and the negative control were obtained in the same day, using the same cells. This may suggest that this pattern appearing in all these wells except in the ones that were obtained in a different day with different cells, may be due to some other components of the supernatant. This result seems to occur due to the low specificity of the anti-HA antibody.

Different anti-HA antibodies were tested and the best one was selected as previously mentioned in section 3.6. However, comparing Figure 21 and Figure 22, it can be observed that, even using the same samples, the patterns in Figure 22 did not appear in Figure 21. This shows that when using this antibody, we cannot achieve reproducible results.

Taking into account the results on the Western blot (Figure 22) and the lack of reproducibility in the results obtained using this antibody, it is necessary to confirm if the band near the 47 kDa is in fact due to the presence of scFv-HER2_gp41 protein and not due to another protein with a similar molecular weight. In order to confirm the presence of the scFv-HER2_gp41 protein in the VLP, we suggest running a new Western blot using an anti-gp41 antibody. If the two bands overlap it is possible to say that the bands that were detected with the anti-HA antibody also have the gp41 protein, so it can be conclusive of the presence of the scFv-HER2_gp41 protein in the VLP.

3.8. HIV-1 based VLP production and quantification for binding assay

In order to incubate the cells, SK-BR-3 and MDA-MB-231, with the HIV-1 based VLPs and analyse them through flow cytometry, a GFP plasmid had to be introduced in the transfection protocol. By adding this new vector to the transfection, the GFP genetic information will be incorporate in the HIV-1 based VLP genome. This new protocol gives rise to a VLP that will transport the GFP genetic information into the cells if internalized. If the HIV-1 based VLP binds to the receptor and is internalized, then the GFP genetic information will be integrated into the cell genome, and the cell will start expressing the GFP.

Batches 8 to 11 followed the transfection protocol presented in section 2.6.5.

The p24 concentration of batches 8 to 11 was calculated as in section 3.1., with equation (7). The results are presented in Table 7.

$$y = -0.0122x^2 + 9.3562x + 89.0770 \quad \textbf{(7)}$$

R^2=0.9986

Table 7: p24 concentration of the HIV-1 based VLP produced by the protocol presented in section 2.6.5.

	pX1655: pMDLg/pRRE: pRSV-REV: pHR_EGFPligand ratio	**[p24] (ng/mL)**
Batch 8	1:1:1:1	0.53
Batch 9	5:1:1:1	0.61
Batch 10	1:1:1:1	0.46
Batch 11	5:1:1:1	0.96

The results presented in Table 7 show again, that different ratios of the pX1665 do not affect the production of the HIV-1 based VLPs. Batches 4, 8 and 10 have a pX1665 ratio of 1. Comparing the batch that was produced with gag-pol and rev (batch 4: 1.41 ng/mL) and the ones where we also added GFP (batches 8 and 10), it can be observed that the production of HIV-1 based VLPs decreased in the later. This may be due to the fact that in both protocols the same amount of DNA is added (3 µg) but on batches 8 and 10 the GFP plasmid was added to the transfection, which means that a smaller quantity

of gag was added compared to batch 4. Since the gag gene is the one that expresses the Gag polyprotein that self-assembles and forms the VLPs, it was already expected a decrease in VLP concentration. The same happens for batches 6 (0.81 ng/mL), 9 and 11, that have a pX1665 ratio of 5. To increase the VLP concentration in the batches that contain VLPs with GFP, we suggest the increase in the ratio of the gag plasmid.

To assess whether assembly of the Gag VLP with the scFv-HER2_gp41 fusion protein was successful, we ran a Western blot protocol with the supernatant (Figure 24).

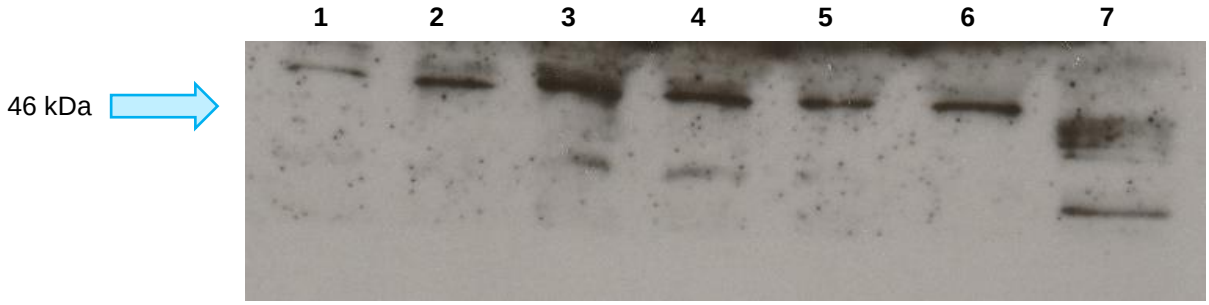

Figure 24: Western blot analysis. 1: batch 4; 2: batch 6; 3: batch 8; 4: batch 9; 5: batch 10; 6: batch 11; 7: positive control (protein extract containing HA). Western blot detection was performed using a Biolegend primary monoclonal HA-antibody (1:2000) and a BioRad secondary antibody anti-mouse (1:3000). Visualization of bands was carried out using the ECL® reagent.

The molecular weight of the protein expressed by the cells is about 46 kDa (Figure 24), slightly lower than the theoretical value. These results confirm the presence of the scFv-HER2_gp41 protein in the HIV-1 based VLP produced in section 2.6.5.

Table 8: Estimated quantity of p24 added to each well in the SDS-PAGE.

	Batch 4	Batch 6	Batch 8	Batch 9	Batch 10	Batch 11
p24 (pg)	21.13	21.10	18.65	21.37	16.17	33.51

Despite the fact that batches 8 to 11 had a lower concentration of p24 than batches 4 and 6 (Table 7 and Table 6, respectively), the amount of scFv-HER2_gp41 protein seems to be higher. Looking at the bands from batches 8 and 9, which were produced on the same day with different ratios of pX1665, 1 and 5, respectively, batch 8 had a lower amount of p24 (Table 8) but the band intensity is slightly higher than batch 9. This result reveals that there are no changes in the production of VLPs expressing the scFv-HER2_gp41 fusion protein with changing the ratio of the pX1665 plasmid. Further studies need to be done to evaluate the role of the pX1665 ratio in the formation of VLPs containing the fusion protein.

3.9. Comparison of the different transfections

In this section a head-to-head comparison of the concentration of HIV-1 VLPs between the different transfection protocols and what their influence is on the efficiency of VLPs production will be made.

Table 9 shows the main differences in the different protocols.

Table 9: Summary of the main differences in the different transfection protocols.

Batch	**Cells/well (10^6)**	**p24 concentration (pg/mL)**	**mass (pMDLg/pRRE)/ number of cells (µg/(10^6cells))**	**Type of transfection**		**Cell Passage**
				x1665+gag-pol+rev ratio	plasmid size	
1	7	3.88	3.00	1:1:0	n/a	13
2	6	$1.94x10^5$	2.92	1:1:1	n/a	23
3	6	$3.36x10^4$	2.92	1:1:1	n/a	27
4	1	$1.41x10^3$	1.35	1:1:1	yes	27
5	1	$1.24x10^3$	1.01	2:1:1	yes	27
6	1	$8.05x10^2$	0.57	5:1:1	yes	27
7	1	$1.26x10^3$	0.33	10:1:1	yes	27
8	1	$5.33x10^2$	0.90	1:1:1*	yes	20
9	1	$6.11x10^2$	0.47	5:1:1*	yes	20
10	1	$4.62x10^2$	0.90	1:1:1*	yes	22
11	1	$9.58x10^2$	0.47	5:1:1*	yes	22

*GFP plasmid added with a ratio of one.

Comparing the different batches, batches 2 and 3 have the highest amount of HIV-1 VLPs produced with p24 concentration of $1.94x10^5$ pg/mL and $3.36x10^4$ pg/mL, respectively. These results are related to the higher amount of pMDLg/pRRE used in both transfection protocols (Table 9). Compared to the other batches, there are some cases such as batches 9 and 11 where up to 6 times less gag-pol plasmid was added. These results confirm that the amount of the pMDLg/pRRE plasmid is a limiting and fundamental feature for the efficient production of VLPs.

By comparing the batches with the highest concentration of p24, batches 2 and 3, it is observed that batch 2 has almost six times more p24 than batch 3. The difference between the transfection protocols of these two batches is the number of cell passages and the adherent condition of the cells. Since batches 4 to 7 used the same passage of cells as batch 3, we conclude that, as mentioned before, the cell conditions are a relevant aspect in the efficiency of VLPs production and that in this case the cell passage was irrelevant to the production efficiency.

Despite the differences in the amount of gag-pol plasmid added between batches 4 to 7 (Table 9), when the size of plasmid is considered, the concentration of p24 is similar. For batches 9 to 11, the GFP plasmid was added to the transfection protocol. In this experiment, the plasmid size was also taken into account, and the p24 concentration is similar. Batches 5, 8 and 10 had a similar amount of gag-pol plasmid added, but in batch 5 the production of HIV-1 based VLP is two times higher than in batches 8 and 10. The addition of a new plasmid to the cells in batches 8 and 10 may also have affected the concentration of VLPs produced, and thus a higher ratio of the gag plasmid will be required to overcome this change (Gonelli et al., 2019).The higher the number of plasmids being introduced in the cells, the lower will be the transfection efficiency. These can be observed in Table 9 where the p24 concentration on the batches that were produced with four plasmids is lower than the ones where three plasmids were transfected into the cells.

Looking at Table 9 and taking into account the cells conditions, the results suggest that up to passage 27 the transfection efficiency is not affected.

3.10. HIV-1 based VLP binding to HER2 receptor

Flow cytometry is an advanced instrument for comprehensive analysis of complex populations in a short period of time. This device depends on the elementary laws of physics, such as the laws of fluidics, optics, and electronics. The fundamental principle is related to light scattering and fluorescence emission (Macey, 2007). The data obtained in the flow cytometry can provide information about biochemical, biophysical and molecular aspects of the particles that are analysed in the cytometer (Adan et al., 2017). This method can measure the optical and fluorescence characteristics of a single cell or other particle. Different parameters are assessed to analyse and differentiate the cell population, like size, granularity and fluorescent features of the cells. Flow cytometry can also gather information on different cellular

processes, as expression of surface markers, intracellular cytokine and signalling proteins, or cell cycle (Jahan-Tigh et al., 2012).

To assess if the HIV-1 based VLPs had the fusion protein on the surface and if the scFv bound to HER2 receptor in the cells and was internalized, flow cytometry was performed. Firstly, the HIV-1 based VLPs were produced as described in section 2.6.5. This means that, if the HIV-1 based VLP binds to HER2 receptor and is internalized into the cell, then the GFP genetic information will be integrated into the cell genome, and the cell will start expressing the GFP. Then, the SK-BR-3 (HER2-positive) and the MDA-MB-231 (HER-2 negative) cells were incubated with the produced HIV-1 based VLPs and analysed by flow cytometry. If the sample with SK-BR-3 cells was GFP positive, it would mean that the HIV-1 based VLPs has bound to the HER2 receptor in the cells. On the contrary, if the sample with MDA-MB-231 cells was GFP negative, it would mean that the HIV-1 based VLPs did not bind to any receptor other than the HER2 receptor (only present in the SK-BR-3).

The data was acquired on the cytometer, and then analysed in the FlowJo software.

To evaluate the cells fluorescence, it was necessary to select the population of interest. First, we plot the FSC (forward scatter) versus SSC (side scatter), where the FSC is related with the cell size and the SSC with the cell complexity, as shown in Figure 25 Left. When the FSC and SSC are low it means that the events are small with extremely low complexity, which means they are cellular debris and should not be taken into account when choosing the population of interest. When the SSC is high but the FSC is low, it means that they are apoptotic bodies and should also be discarded. The population of interest is selected based on the population that has a higher FSC and an intermediated SSC because the SK- BR-3 and MDA-MB-231 cells have some granules but are not very complex. After selecting the population of interest, we plot the FSC-Area versus FSC-Height, as shown in Figure 25 Right. This plot is used to differentiate single cells from cellular complexes and just select the single cells from the population of interest.

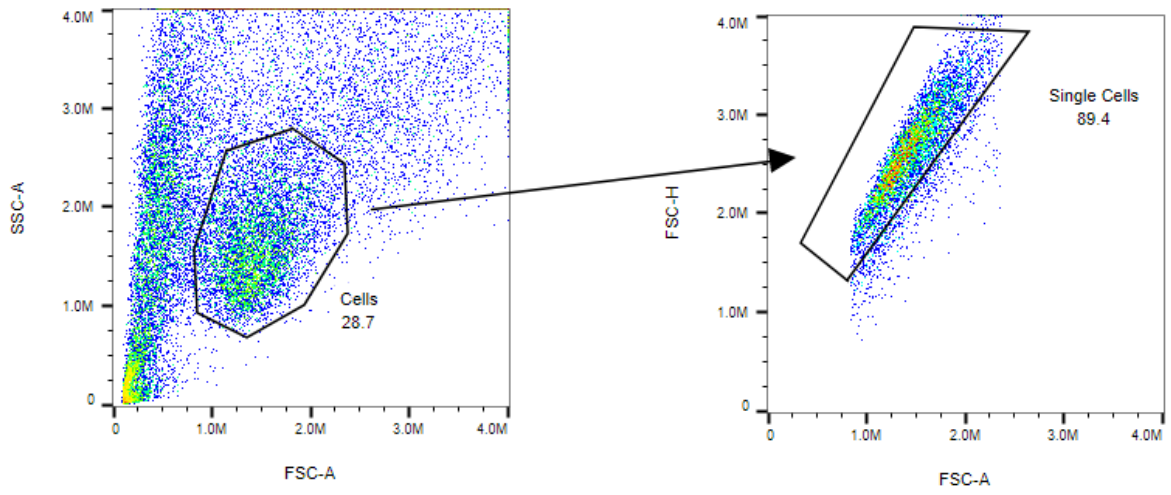

Figure 25: Flow cytometry gating strategy. Left - SSC-A versus FSC-A density plot to select the cells of interest. Right - FSC-H versus FSC-A density plot to select the single cells in the population of interest.

Subsequently, a graph of the GFP intensity versus the number of cells was plotted (Figure 26 to 29) to compare the number of GFP positive cells against the control.

In Figure 26, the results are shown for the SK-BR-3 cells incubated with HIV-1 based VLPs produced with a pX1665 ratio of one. It can be observed a shift of fluorescence from left to right and an increase in the GFP positive population in the samples that were incubated with the VLPs.

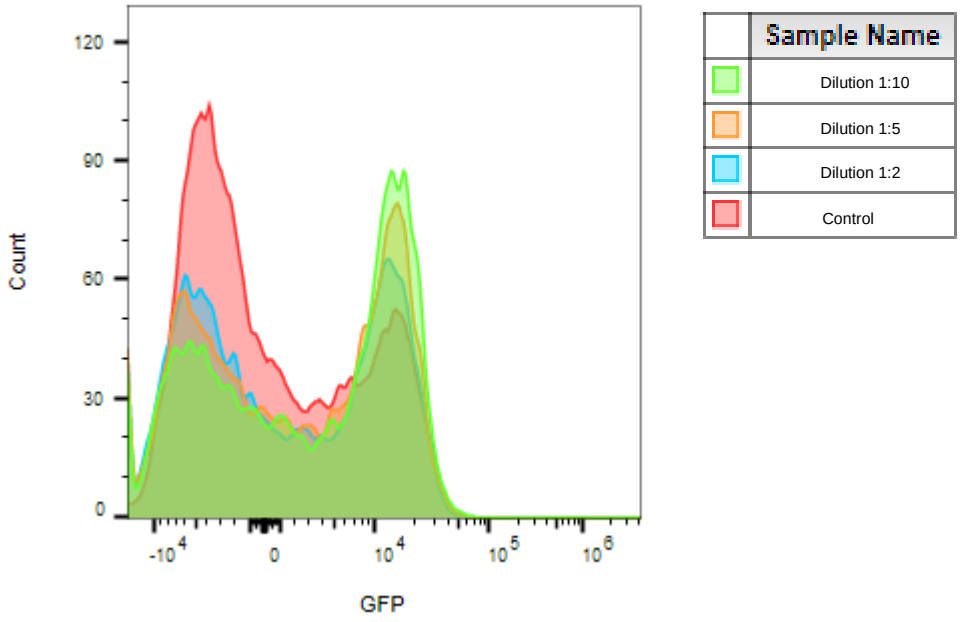

Figure 26: Assessment of GFP presence in the SK-BR-3 cells incubated with HIV-1 based VLPs (batch 8 - pX1665 ratio of one).

The samples that were incubated with the HIV-1 based VLPs are more GFP positive than the control group, which may suggest that the VLPs bound to the SK-BR-3 and were able to internalize in these cells. It is also observed that, when a higher dilution was used to incubate the cells, an increase in the population (number of cells) that are GFP positive occurred. These results may be due to the fact that a higher quantity of VLPs entering the cells, and integrating the GFP genetic information in the cell genome, can translate in a higher cell death, which decreases the amount of fluorescence obtained in the flow cytometer. Further, in Figure 26, the control group has a peak which occurs due to the auto fluorescence present in this sample. This auto fluorescence may be caused by the presence of dead cells in the population selected. To confirm and remove the dead cells from the population of interest, a viability dye must be added to the samples.

In Figure 27, the results for the SK-BR-3 incubated with HIV-1 based VLPs produced with a pX1665 ratio of five are presented. It can also be observed a shift of fluorescence from left to right and an increase in the GFP positive population in the samples that were incubated with the VLPs, which means that the VLPs bound to the SK-BR-3 and were able to internalize these cells.

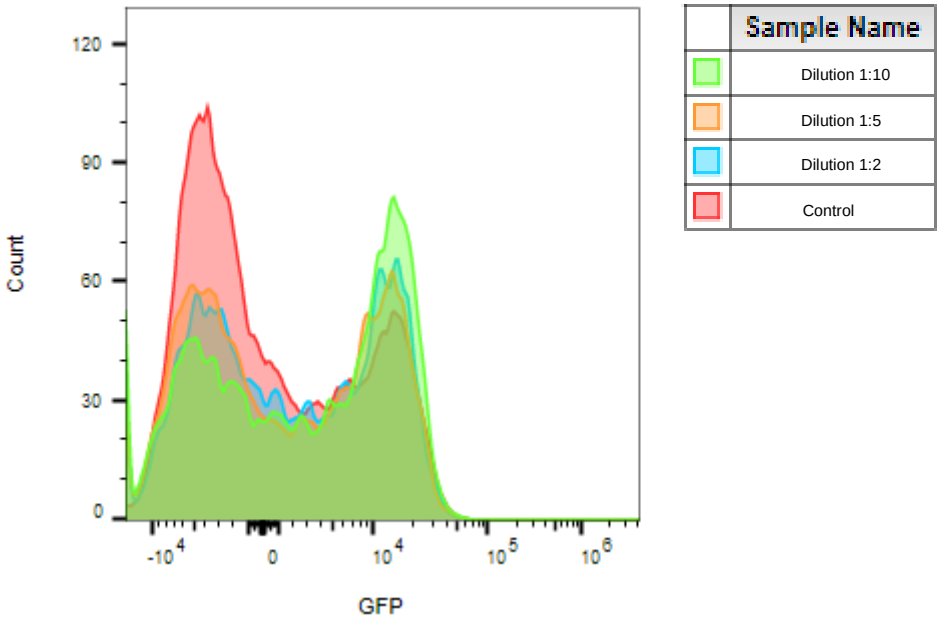

Figure 27: Assessment of GFP presence in the SK-BR-3 cells incubated with HIV-1 based VLPs (batch 9 - pX1665 ratio of five).

In the samples incubated with HIV-1 based VLPs produced with a pX1665 ratio of five (Figure 27), it can be observed that there is a smaller population of GFP positive cells, which means it did not bind as much as in the ones incubated with the VLPs produced with a ratio of one (Figure 26). This suggests that using this ratio in the transfection, may lead to a reduction in the production of competent VLPs. These results indicate that producing HIV-1 based VLPs with a pX1665 ratio of five may not bring any advantage compared to a ratio of one.

Figure 28 displays the results for the MDA-MB-231 incubated with HIV-1 based VLPs produced with a pX1665 ratio of one.

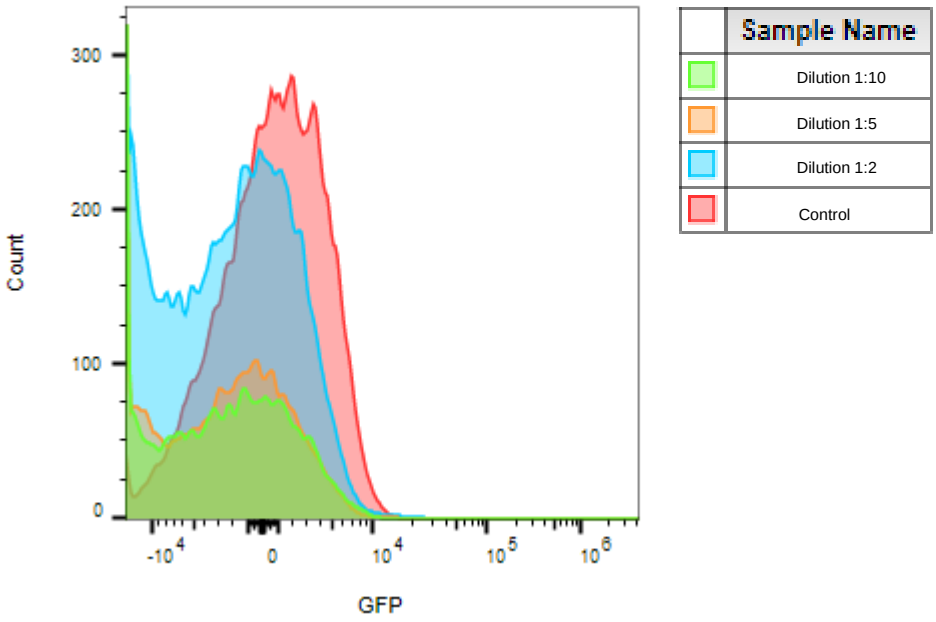

Figure 28: Assessment of GFP presence in the MDA-MB-231 cells incubated with HIV-1 based VLPs (batch 8 - pX1665 ratio of one).

In this condition, the control group has the population with the highest GFP intensity which may imply that the VLPs did not bind to the MDA-MB-231 cells.

Figure 29 shows the results for the MDA-MB-231 incubated with HIV-1 based VLPs produced with a pX1665 ratio of five. In Figure 29, it can be observed that all the samples have a GFP intensity lower than the control group, which suggests that VLPs from batch 9 also did not bind to the MDA-MB-231 cells.

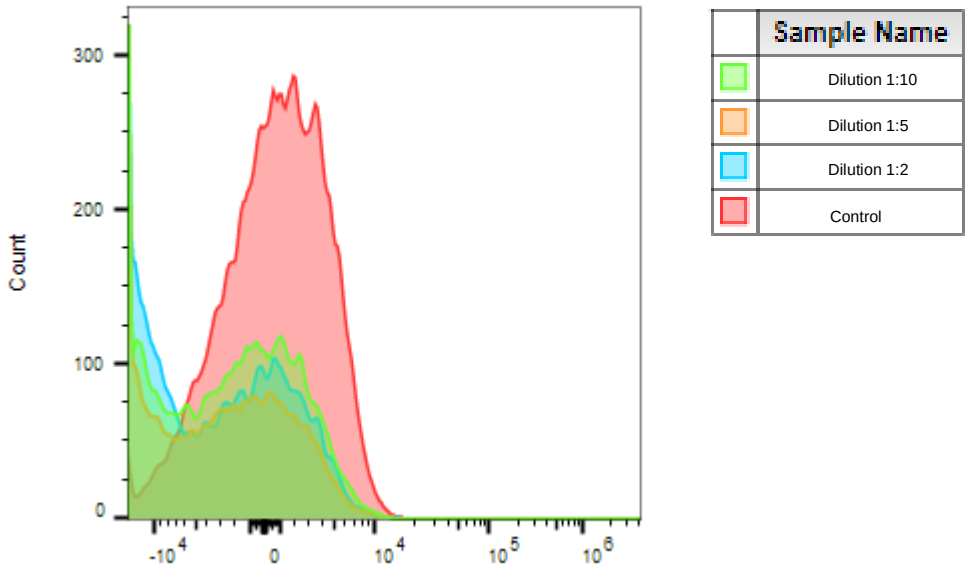

Figure 29: Assessment of GFP presence in the MDA-MB-231 cells incubated with HIV-1 based VLPs (batch 9 - pX1665 ratio of five).

These preliminary results suggest that the HIV-1 based VLPs produced bound to the HER2 receptor of the SK-BR-3 cells and they did not bind to any other receptor as seen with MDA-MB-231 cells. It indicates that there is specificity between the VLP and the HER2 receptor of the SK-BR-3 cells as it was predicted by our team based on *in silico* studies. Nevertheless, future optimizations to the process must be done and these results should be verified.

3.11. Evaluation of cytotoxic effect

One important aspect that is necessary to analyse when working with nanoparticles is the cytotoxic effect they can have in the proliferation of cells. For this reason, a cytotoxicity assay, WST-1 proliferation test, was done. In this assay, an increase in the number of viable cells can be seen due to an increase in the amount of formazan dye formed as a result of the cleavage of tetrazolium salts added to the medium caused by the mitochondrial dehydrogenase activity in the viable cells.

The proliferation of cells incubated with the produced HIV-1 based VLPs was compared with the proliferation of cells that were not incubated. The cells chosen for this assay were the SK-BR-3 cells because they overexpress the HER2 receptor on their membranes and as was seen in the cytometry the VLPs bind to this receptor in these cells.

The cell viability was calculated by Equation (8) and the results are presented in Table 10.

$$\%\ Cell\ Viability = \frac{Absorbance_{Incubated\ cells} - Absorbance_{VLPs}}{Absorbance_{Not\ incubated\ cells} - Absorbance_{Culture\ Medium}} \times 100\% \quad \textbf{(8)}$$

Table 10: Fraction cell viability of the cytotoxic assay samples.

	Fraction cell viability	
	Assay 1	Assay 2
Cells incubated with batch 8 dilution 1/2	1.60	0.99
Cells incubated with batch 8 dilution 1/5	1.55	1.04
Cells incubated with batch 8 dilution 1/10	1.56	1.13
Cells incubated with batch 9 dilution 1/2	1.41	1.16
Cells incubated with batch 9 dilution 1/5	1.45	1.17
Cells incubated with batch 9 dilution 1/10	1.67	1.13

Figure 30 shows that the cell viability has increased when compared to the untreated cells (cells not incubated with the VLPs), which indicates that the VLPs produced are not cytotoxic to the cells.

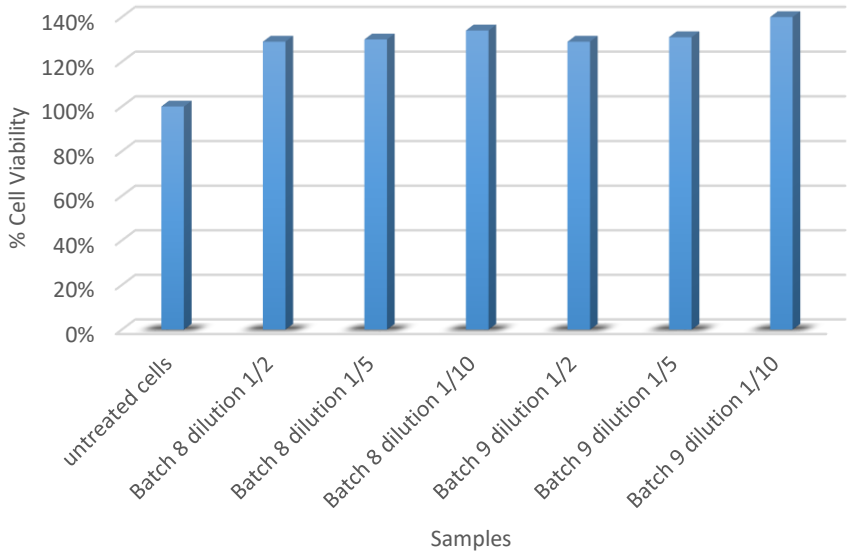

Figure 30: Cell viability of SK-BR-3 cells after incubation with HIV-1 based VLPs produced in section 2.6.5.

The difference between the different batches results is not significant to conclude that incubating the cells with VLPs produced with distinct ratios of pX1665 will have different cytotoxic effects on the cells. However, the difference between the cell viability of incubated and not incubated cells is around 30%, higher than the 10% value that is acceptable due to random experimental fluctuations. This result may indicate that the addition of the VLPs to the cells stimulated the cell growth. The main difference between incubated and not incubated cells is the medium. Untreated cells were in fresh medium (DMEM 10%FBS), while the incubated cells also had the spent medium of the HEK-293T cells where the VLPs were produced and collected. Despite the step of centrifugation where cell debris are removed from the supernatant that contains the VLPs, this supernatant can have exosomes, growth factors and other molecules from the HEK-293T cells that may influence the cellular growth of the SK-BR-3 cells. Beas-Catena studied the effect of spent medium on cell proliferation and concluded that when less than 50% of spent medium from a culture in mid-exponential growth phase is used, it improves the cellular growth when compared to the control culture grown in fresh medium (Beas-Catena et al., 2013).

To validate the results obtained, it is necessary to repeat the experiment changing the supernatant where the VLPs are to PBS, for example, so the effect of the spent medium in the viability of the SK- BR- 3 cells can be eliminated.

4. Conclusions and Future Perspectives

Virus-Like Particles are a novelty nanoplatform to be used as drug delivery systems due their biocompatibility and biodegradability (Steinmetz, 2010).

The work presented in this thesis showed that it is possible to produce an HIV-1 based VLP containing on the surface a scFv of an anti-HER2 antibody with specificity to the target receptor HER2 and that is not cytotoxic to the cells.

Firstly, we demonstrated that the design plasmid construction (pX1665) is robust and can be expressed in HEK-293T cells (Santos et al., 2021).

Moreover, we were able to produce HIV-1 based VLPs in mammalian HEK-293T cell cultures using a transient transfection method with Lipofectamine™ 3000. Our results revealed that the plasmid encoding the Rev protein (pRSV-REV), which modulates gag transcription, is critical for higher yields in the production of HIV-1 based VLPs. Additionally, it was found that the concentration of p24 is greatly influenced by the quantity of pMDLg/pRRE plasmid, playing a critical role in the efficient production of HIV-1 based VLPs. On the other hand, increasing the ratio of pX1665 in the transfection protocol does not translate into increased production of HIV-1 based VLPs containing the anti-HER2 scFV. Furthermore, the higher the number of plasmids being transfected in the cells, the lower the transfection efficiency. For example, if the VLPs need to be labelled with GFP, then a higher ratio of the gag plasmid may be needed to overcome this addition. The plasmids are not the only factor that affects the transfection efficiency. Indeed, the optimization of the cell density is important because the transfection efficiency decreases substantially at higher cell densities (Cervera et al., 2019). Besides, we also observed that the adherence condition of the transfected cells has great influence on production yields.

In the Western blot assays, we found some issues regarding anti-HA antibodies due to their low specificity which leads to a lack of reproducible results. This makes it necessary to confirm the results obtained by this technique with another antibody.

Preliminary results suggest that the HIV-1 based VLPs bind to HER2 expressed by SK-BR-3 cell line and, in addition, have some specificity since they did not bind to MDA-MB-231 cell line (HER2 negative). Subsequently, the cytotoxic assay showed that the HIV-1 based VLPs are not cytotoxic to the cells.

Overall, the results presented in this thesis validated a new approach for targeted therapy using recombinant proteins to be expressed into VLPs that can be designed by *in silico* methods.

From the results obtained in this thesis, it is necessary to confirm the presence of the scFv-HER2_gp41 protein using an anti-gp41 antibody in the Western blot. Also, to repeat the cytotoxic assay

and eliminate the effect of the spent medium in the viability of the SK-BR-3 cells, by changing the supernatant where the VLPs are to PBS.

As a next step, it would be interesting to characterize the morphology of the HIV-1 based VLP containing at the surface a scFv of an anti-HER2 antibody by performing a TEM analysis and also by comparing it to a Gag VLP. Further, we suggest the improvement of the VLP production by studying different ratios of the pMDLg/pRRE or changing the packaging vector. Moreover, the flow cytometry protocol should be optimized and more dilutions of the HIV-1 based VLPs should be studied.

In the future, it would be important to study the specificity of the HIV-1 based VLP *in vivo* and additionally, to evaluate different purification methods to obtain a more concentrated and cleaner sample.

5. References

Adan, A., Alizada, G., Kiraz, Y., Baran, Y., & Nalbant, A. (2017). Flow cytometry: basic principles and applications. *Critical Reviews in Biotechnology*, *37*(2), 163–176. https://doi.org/10.3109/07388551.2015.1128876

Advani, P. P., Crozier, J. A., & Perez, E. A. (2015). HER2 testing and its predictive utility in anti-HER2 breast cancer therapy. *Biomarkers in Medicine*, *9*(1), 35–49. https://doi.org/10.2217/bmm.14.95

Agus, D. B., Akita, R. W., Fox, W. D., Lewis, G. D., Higgins, B., Pisacane, P. I., Lofgren, J. A., Tindell, C., Evans, D. P., Maiese, K., Scher, H. I., & Sliwkowski, M. X. (2002). Targeting ligand-activated ErbB2 signaling inhibits breast and prostate tumor growth. *Cancer Cell*, *2*(2), 127–137. https://doi.org/10.1016/s1535-6108(02)00097-1

Agus, D. B., Gordon, M. S., Taylor, C., Natale, R. B., Karlan, B., Mendelson, D. S., Press, M. F., Allison, D. E., Sliwkowski, M. X., Lieberman, G., Kelsey, S. M., & Fyfe, G. (2005). Phase I clinical study of pertuzumab, a novel HER dimerization inhibitor, in patients with advanced cancer. *Journal of Clinical Oncology : Official Journal of the American Society of Clinical Oncology*, *23*(11), 2534–2543. https://doi.org/10.1200/JCO.2005.03.184

Alexis, F., Basto, P., Levy-Nissenbaum, E., Radovic-Moreno, A. F., Zhang, L., Pridgen, E., Wang, A. Z., Marein, S. L., Westerhof, K., Molnar, L. K., & Farokhzad, O. C. (2008). HER-2-targeted nanoparticle-affibody bioconjugates for cancer therapy. *ChemMedChem*, *3*(12), 1839–1843. https://doi.org/10.1002/cmdc.200800122

Aljabali, A. A. A., Alzoubi, L., Hamzat, Y., Alqudah, A., Obeid, M. A., Al Zoubi, M. S., Ennab, R. M., Alshaer, W., Albatayneh, K., Al-Trad, B., Alqudah, D. A., Chellappan, D. K., Gupta, G., Tambuwala, M. M., Kamal, D., & Evans, D. J. (2020). A potential MRI agent and an anticancer drug encapsulated within CPMV virus-like particles. *Combinatorial Chemistry & High Throughput Screening*, *24*(10), 1557–1571. https://doi.org/10.2174/1386207323666200914110012

Bachmann, M F, Rohrer, U. H., Kündig, T. M., Bürki, K., Hengartner, H., & Zinkernagel, R. M. (1993). The influence of antigen organization on B cell responsiveness. *Science (New York, N.Y.)*, *262*(5138), 1448–1451. https://doi.org/10.1126/science.8248784

Bachmann, Martin F, & Dyer, M. R. (2004). Therapeutic vaccination for chronic diseases: a new class of drugs in sight. *Nature Reviews Drug Discovery*, *3*(1), 81–88. https://doi.org/10.1038/nrd1284

Bachmann, Martin F, & Zinkernagel, R. M. (1997). Neutralizing Antiviral. *Annu. Rev. Immunol.*, *15*, 235–270. https://doi.org/doi:10.1146/annurev.immunol.15.1.235

Beas-Catena, A., Sánchez-Mirón, A., García-Camacho, F., Contreras-Gómez, A., & Molina-Grima, E. (2013). The effect of spent medium recycle on cell proliferation, metabolism and baculovirus

production by the lepidopteran Se301 cell line infected at very low MOI. *Journal of Microbiology and Biotechnology*, *23*(12), 1747–1756. https://doi.org/10.4014/jmb.1305.05067

Bednarska, J., Pelchen-Matthews, A., Novak, P., Burden, J. J., Summers, P. A., Kuimova, M. K., Korchev, Y., Marsh, M., & Shevchuk, A. (2020). Rapid formation of human immunodeficiency virus-like particles. *Proceedings of the National Academy of Sciences of the United States of America*, *117*(35), 21637–21646. https://doi.org/10.1073/pnas.2008156117

Benjamin, J., Ganser-Pornillos, B. K., Tivol, W. F., Sundquist, W. I., & Jensen, G. J. (2005). Three-dimensional structure of HIV-1 virus-like particles by electron cryotomography. *Journal of Molecular Biology*, *346*(2), 577–588. https://doi.org/10.1016/j.jmb.2004.11.064

Beyer, T., Herrmann, M., Reiser, C., Bertling, W., & Hess, J. (2001). Bacterial carriers and virus-like-particles as antigen delivery devices: role of dendritic cells in antigen presentation. *Current Drug Targets. Infectious Disorders*, *1*(3), 287–302. https://doi.org/10.2174/1568005014605973

Brouwer, P. J. M., & Sanders, R. W. (2019). Presentation of HIV-1 envelope glycoprotein trimers on diverse nanoparticle platforms. *Current Opinion in HIV and AIDS*, *14*(4), 302–308. https://doi.org/10.1097/COH.0000000000000549

Buonaguro, L., Tagliamonte, M., Visciano, M. L., Tornesello, M. L., & Buonaguro, F. M. (2013). Developments in virus-like particle-based vaccines for HIV. *Expert Review of Vaccines*, *12*(2), 119–127. https://doi.org/10.1586/erv.12.152

Caldeira, J. C., Perrine, M., Pericle, F., & Cavallo, F. (2020). Virus-Like Particles as an Immunogenic Platform for Cancer Vaccines. *Viruses*, *12*(5). https://doi.org/10.3390/v12050488

Cameron, D. A., & Stein, S. (2008). Drug Insight: intracellular inhibitors of HER2--clinical development of lapatinib in breast cancer. *Nature Clinical Practice. Oncology*, *5*(9), 512–520. https://doi.org/10.1038/ncponc1156

Cervera, L., Gòdia, F., Tarrés-Freixas, F., Aguilar-Gurrieri, C., Carrillo, J., Blanco, J., & Gutiérrez-Granados, S. (2019). Production of HIV-1-based virus-like particles for vaccination: achievements and limits. *Applied Microbiology and Biotechnology*, *103*(18), 7367–7384. https://doi.org/10.1007/s00253-019-10038-3

Cervera, L., Gutiérrez-Granados, S., Martínez, M., Blanco, J., Gòdia, F., & Segura, M. M. (2013). Generation of HIV-1 Gag VLPs by transient transfection of HEK 293 suspension cell cultures using an optimized animal-derived component free medium. *Journal of Biotechnology*, *166*(4), 152–165. https://doi.org/10.1016/j.jbiotec.2013.05.001

Charlton Hume, H. K., & Lua, L. H. L. (2017). Platform technologies for modern vaccine manufacturing. *Vaccine*, *35*(35 Pt A), 4480–4485. https://doi.org/10.1016/j.vaccine.2017.02.069

Chen, C., Saubi, N., & Joseph-munné, J. (2020). *Design Concepts of Virus-Like Particle-Based HIV-1 Vaccines*. *11*(September), 1–8. https://doi.org/10.3389/fimmu.2020.573157

Chroboczek, J., Szurgot, I., & Szolajska, E. (2014). *Virus-like particles as vaccine*. *61*(3), 531–539.

Dai, X., Cheng, H., Bai, Z., & Li, J. (2017). Breast Cancer Cell Line Classification and Its Relevance with Breast Tumor Subtyping. *Journal of Cancer*, *8*(16), 3131–3141. https://doi.org/10.7150/jca.18457

Deml, L., Speth, C., Dierich, M. P., Wolf, H., & Wagner, R. (2005). Recombinant HIV-1 Pr55gag virus-like particles: potent stimulators of innate and acquired immune responses. *Molecular Immunology*, *42*(2), 259–277. https://doi.org/10.1016/j.molimm.2004.06.028

Dhritlahre, R. K., & Saneja, A. (2021). Recent advances in HER2-targeted delivery for cancer therapy. *Drug Discovery Today*, *26*(5), 1319–1329. https://doi.org/10.1016/j.drudis.2020.12.014

Dietmair, S., Hodson, M. P., Quek, L.-E., Timmins, N. E., Gray, P., & Nielsen, L. K. (2012). A multi-omics analysis of recombinant protein production in Hek293 cells. *PloS One*, *7*(8), e43394. https://doi.org/10.1371/journal.pone.0043394

Dull, T., Zufferey, R., Kelly, M., Mandel, R. J., Nguyen, M., Trono, D., & Naldini, L. (1998). A third-generation lentivirus vector with a conditional packaging system. *Journal of Virology*, *72*(11), 8463–8471. https://doi.org/10.1128/JVI.72.11.8463-8471.1998

Faltus, T., Yuan, J., Zimmer, B., Krämer, A., Loibl, S., Kaufmann, M., & Strebhardt, K. (2004). Silencing of the HER2/neu gene by siRNA inhibits proliferation and induces apoptosis in HER2/neu-overexpressing breast cancer cells. *Neoplasia (New York, N.Y.)*, *6*(6), 786–795. https://doi.org/10.1593/neo.04313

Fernandes, B., Vidigal, J., Correia, R., Carrondo, M. J. T., Alves, P. M., Teixeira, A. P., & Roldão, A. (2020). Adaptive laboratory evolution of stable insect cell lines for improved HIV-Gag VLPs production. *Journal of Biotechnology*, *307*, 139–147. https://doi.org/10.1016/j.jbiotec.2019.10.004

Fink, S. L., & Campbell, S. (2018). Infection and host response. In *Molecular Pathology: The Molecular Basis of Human Disease* (pp. 45–69). Elsevier Inc. https://doi.org/10.1016/B978-0-12-802761-5.00003-1

Flexman, J. A., Cross, D. J., Lewellen, B. L., Miyoshi, S., Kim, Y., & Minoshima, S. (2008). *Magnetically Targeted Viral Envelopes : A PET Investigation of Initial Biodistribution*. *7*(3), 223–232.

Forouhar-Kalkhoran, B. (2017). A Short Review on Virus-Like Particles as Vaccine and Delivery Systems. *Journal of Molecular Biology and Genetics*, *2*(May), 53–59.

Franklin, M. C., Carey, K. D., Vajdos, F. F., Leahy, D. J., de Vos, A. M., & Sliwkowski, M. X. (2004). Insights into ErbB signaling from the structure of the ErbB2-pertuzumab complex. *Cancer Cell*, *5*(4), 317–328. https://doi.org/10.1016/s1535-6108(04)00083-2

Fuenmayor, J, Gòdia, F., & Cervera, L. (2017). Production of virus-like particles for vaccines. *New BIOTECHNOLOGY*, *39*, 174–180. https://doi.org/10.1016/j.nbt.2017.07.010

Fuenmayor, Javier, Cervera, L., Gutiérrez-Granados, S., & Gòdia, F. (2018). Transient gene expression optimization and expression vector comparison to improve HIV-1 VLP production in HEK293 cell lines. *Applied Microbiology and Biotechnology*, *102*(1), 165–174. https://doi.org/10.1007/s00253-017-8605-x

Fuenmayor, Javier, Cervera, L., Rigau, C., & Gòdia, F. (2018). Enhancement of HIV-1 VLP production using gene inhibition strategies. *Applied Microbiology and Biotechnology*, *102*(10), 4477–4487. https://doi.org/10.1007/s00253-018-8930-8

García, J. L., Jorge, I., Besora, A. B., Vázquez, J., Gòdia, F., & Cervera, L. (2021). *Characterization of HIV - 1 virus - like particles and determination of Gag stoichiometry for different production platforms*. https://doi.org/10.1002/bit.27786

Garg, H., & Blumenthal, R. (2008). Role of HIV Gp41 mediated fusion/hemifusion in bystander apoptosis. *Cellular and Molecular Life Sciences : CMLS*, *65*(20), 3134–3144. https://doi.org/10.1007/s00018-008-8147-6

Gerber, D. E. (2008). Targeted therapies: a new generation of cancer treatments. *American Family Physician*, *77*(3), 311–319.

Gharagozloo, M., Kalantari, H., Rezaei, A., Maracy, M. R., Salehi, M., Bahador, A., Hassannejad, N., Narimani, M., Sanei, M. H., Bayat, B., & Ghazanfari, H. (2015). Comparison of transfection effi ciency of polymer-based and lipid-based transfection reagents. *Bratislavsk?? Lek??Rske Listy*, *116*(5), 296–301. https://doi.org/10.4149/BLL

Gonelli, C. A., Khoury, G., Center, R. J., & Purcell, D. F. J. (2019). HIV-1-Based Virus-like Particles that Morphologically Resemble Mature, Infectious HIV-1 Virions. In *Viruses* (Vol. 11, Issue 6). https://doi.org/10.3390/v11060507

González-Domínguez, I., Gutiérrez-Granados, S., Cervera, L., Gòdia, F., & Domingo, N. (2016). Identification of HIV-1-Based Virus-like Particles by Multifrequency Atomic Force Microscopy. *Biophysical Journal*, *111*(6), 1173–1179. https://doi.org/10.1016/j.bpj.2016.07.046

González-Domínguez, I., Puente-Massaguer, E., Cervera, L., & Gòdia, F. (2020). Quantification of the HIV-1 virus-like particle production process by super-resolution imaging: From VLP budding to nanoparticle analysis. *Biotechnology and Bioengineering*, *117*(7), 1929–1945. https://doi.org/10.1002/bit.27345

Gulati, N. M., Stewart, P. L., & Steinmetz, N. F. (2018). Bioinspired Shielding Strategies for Nanoparticle Drug Delivery Applications. In *Molecular Pharmaceutics* (Vol. 15, Issue 8, pp. 2900–2909). American Chemical Society. https://doi.org/10.1021/acs.molpharmaceut.8b00292

Gutiérrez-Granados, S., Cervera, L., Gòdia, F., Carrillo, J., & Segura, M. M. (2013). Development and validation of a quantitation assay for fluorescently tagged HIV-1 virus-like particles. *Journal of Virological Methods*, *193*(1), 85–95. https://doi.org/10.1016/j.jviromet.2013.05.010

Gutiérrez-Granados, S., Cervera, L., Segura, M. de L. M., Wölfel, J., & Gòdia, F. (2016). Optimized production of HIV-1 virus-like particles by transient transfection in CAP-T cells. *Applied Microbiology and Biotechnology*, *100*(9), 3935–3947. https://doi.org/10.1007/s00253-015-7213-x

Gutiérrez-Granados, S., Farràs, Q., Hein, K., Fuenmayor, J., Félez, P., Segura, M., & Gòdia, F. (2017). Production of HIV virus-like particles by transient transfection of CAP-T cells at bioreactor scale avoiding medium replacement. *Journal of Biotechnology*, *263*, 11–20. https://doi.org/10.1016/j.jbiotec.2017.09.019

Han-Chung, W., Chang, D.-K., & Chia-Ting, H. (2006). Targeted Therapy for Cancer. *Journal of Cancer Molecules*, *2*.

Hest, J. C. M. Van, Cornelissen, J. J. L. M., & Koay, M. S. T. (2014). *Using viruses as nanomedicines*. 4001–4009. https://doi.org/10.1111/bph.12662

Hooker, J. M., Neil, J. P. O., Romanini, D. W., Taylor, S. E., & Francis, M. B. (2008). *Genome-free Viral Capsids as Carriers for Positron Emission Tomography Radiolabels*. *April*, 182–191. https://doi.org/10.1007/s11307-008-0136-5

Iqbal, N., & Iqbal, N. (2014). Human Epidermal Growth Factor Receptor 2 (HER2) in Cancers: Overexpression and Therapeutic Implications. *Molecular Biology International*. https://doi.org/10.1155/2014/852748

Jahan-Tigh, R. R., Ryan, C., Obermoser, G., & Schwarzenberger, K. (2012). Flow cytometry. *The Journal of Investigative Dermatology*, *132*(10), 1–6. https://doi.org/10.1038/jid.2012.282

Kim, T. K., & Eberwine, J. H. (2010). Mammalian cell transfection: the present and the future. *Analytical and Bioanalytical Chemistry*, *397*(8), 3173–3178. https://doi.org/10.1007/s00216-010-3821-6

Kushnir, N., Streatfield, S. J., & Yusibov, V. (2012). Virus-like particles as a highly efficient vaccine platform: diversity of targets and production systems and advances in clinical development. *Vaccine*, *31*(1), 58–83. https://doi.org/10.1016/j.vaccine.2012.10.083

Lavado-García, J., Díaz-Maneh, A., Canal-Paulí, N., Pérez-Rubio, P., Gòdia, F., & Cervera, L. (2021). Metabolic engineering of HEK293 cells to improve transient transfection and cell budding of HIV-1 virus-like particles. *Biotechnology and Bioengineering*, *118*(4), 1649–1663. https://doi.org/10.1002/bit.27679

Lavado-García, J., Jorge, I., Cervera, L., Vázquez, J., & Gòdia, F. (2020). Multiplexed Quantitative Proteomic Analysis of HEK293 Provides Insights into Molecular Changes Associated with the Cell Density Effect, Transient Transfection, and Virus-Like Particle Production. *Journal of Proteome Research*, *19*(3), 1085–1099. https://doi.org/10.1021/acs.jproteome.9b00601

Le, D. T., & Müller, K. M. (2021). In Vitro Assembly of Virus-Like Particles and Their Applications. *Life (Basel, Switzerland)*, *11*(4). https://doi.org/10.3390/life11040334

Lee, L. A., Niu, Z., & Wang, Q. (2009). Viruses and virus-like protein assemblies-Chemically programmable nanoscale building blocks. *Nano Research*, *2*(5), 349–364. https://doi.org/10.1007/s12274-009-9033-8

Lee, Y. T., Tan, Y. J., & Oon, C. E. (2018). Molecular targeted therapy: Treating cancer with specificity. *European Journal of Pharmacology*, *834*, 188–196. https://doi.org/https://doi.org/10.1016/j.ejphar.2018.07.034

Lewis Phillips, G. D., Li, G., Dugger, D. L., Crocker, L. M., Parsons, K. L., Mai, E., Blättler, W. A., Lambert, J. M., Chari, R. V. J., Lutz, R. J., Wong, W. L. T., Jacobson, F. S., Koeppen, H., Schwall, R. H., Kenkare-Mitra, S. R., Spencer, S. D., & Sliwkowski, M. X. (2008). Targeting HER2-positive breast cancer with trastuzumab-DM1, an antibody-cytotoxic drug conjugate. *Cancer Research*, *68*(22), 9280–9290. https://doi.org/10.1158/0008-5472.CAN-08-1776

Liu, Y., Majumder, S., McCall, W., Sartor, C. I., Mohler, J. L., Gregory, C. W., Earp, H. S., & Whang, Y. E. (2005). Inhibition of HER-2/neu Kinase Impairs Androgen Receptor Recruitment to the Androgen Responsive Enhancer. *Cancer Research*, *65*(8), 3404 LP – 3409. https://doi.org/10.1158/0008-5472.CAN-04-4292

Lua, L. H. L., Connors, N. K., Sainsbury, F., Chuan, Y. P., Wibowo, N., & Middelberg, A. P. J. (2014). Bioengineering virus-like particles as vaccines. *Biotechnology and Bioengineering*, *111*(3), 425–440. https://doi.org/10.1002/bit.25159

Lynch, A. G., Tanzer, F., Fraser, M. J., Shephard, E. G., Williamson, A.-L., & Rybicki, E. P. (2010). Use of the piggyBac transposon to create HIV-1 gag transgenic insect cell lines for continuous VLP production. *BMC Biotechnology*, *10*, 30. https://doi.org/10.1186/1472-6750-10-30

Ma, Y., Nolte, R. J. M., & Cornelissen, J. J. L. M. (2012). Virus-based nanocarriers for drug delivery ☆. *Advanced Drug Delivery Reviews*, *64*(9), 811–825. https://doi.org/10.1016/j.addr.2012.01.005

Macey, M. G. (2007). Flow cytometry: Principles and applications. In *Flow Cytometry: Principles and Applications*. https://doi.org/10.1007/978-1-59745-451-3

Manolova, V., Flace, A., Bauer, M., Schwarz, K., Saudan, P., & Bachmann, M. F. (2008). Nanoparticles target distinct dendritic cell populations according to their size. *European Journal of Immunology*, *38*(5), 1404–1413. https://doi.org/10.1002/eji.200737984

Maurisse, R., De Semir, D., Emamekhoo, H., Bedayat, B., Abdolmohammadi, A., Parsi, H., & Gruenert, D. C. (2010). Comparative transfection of DNA into primary and transformed mammalian cells from different lineages. *BMC Biotechnology*, *10*, 9. https://doi.org/10.1186/1472-6750-10-9

McKinstry, W. J., Hijnen, M., Tanwar, H. S., Sparrow, L. G., Nagarajan, S., Pham, S. T., & Mak, J. (2014). Expression and purification of soluble recombinant full length HIV-1 Pr55(Gag) protein in Escherichia coli. *Protein Expression and Purification*, *100*, 10–18. https://doi.org/10.1016/j.pep.2014.04.013

Min, X., Zhang, J., Li, R.-H., Xia, F., Cheng, S.-Q., Li, M., Zhu, W., Zhou, W., Li, F., & Sun, Y. (2021). Encapsulation of NIR-II AIEgens in Virus-like Particles for Bioimaging. *ACS Applied Materials & Interfaces*, *13*(15), 17372–17379. https://doi.org/10.1021/acsami.1c02691

Mohsen, M. O., Zha, L., Cabral-Miranda, G., & Bachmann, M. F. (2017). Major findings and recent advances in virus–like particle (VLP)-based vaccines. *Seminars in Immunology*, *34*(September), 123–132. https://doi.org/10.1016/j.smim.2017.08.014

Nahta, R., Yu, D., Hung, M.-C., Hortobagyi, G. N., & Esteva, F. J. (2006). Mechanisms of disease: understanding resistance to HER2-targeted therapy in human breast cancer. *Nature Clinical Practice. Oncology*, *3*(5), 269–280. https://doi.org/10.1038/ncponc0509

Niehans, G. A., Singleton, T. P., Dykoski, D., & Kiang, D. T. (1993). Stability of HER-2/neu expression over time and at multiple metastatic sites. *Journal of the National Cancer Institute*, *85*(15), 1230–1235. https://doi.org/10.1093/jnci/85.15.1230

Nooraei, S., Bahrulolum, H., Hoseini, Z. S., Katalani, C., & Hajizade, A. (2021). Virus - like particles : preparation, immunogenicity and their roles as nanovaccines and drug nanocarriers. *Journal of Nanobiotechnology*, *19*(59), 1–27. https://doi.org/10.1186/s12951-021-00806-7

Padma, V. V. (2015). An overview of targeted cancer therapy. *BioMedicine*, *5*(4), 19. https://doi.org/10.7603/s40681-015-0019-4

Park, J. W., Hong, K., Kirpotin, D. B., Colbern, G., Shalaby, R., Baselga, J., Shao, Y., Nielsen, U. B., Marks, J. D., Moore, D., Papahadjopoulos, D., & Benz, C. C. (2002). Anti-HER2 immunoliposomes: enhanced efficacy attributable to targeted delivery. *Clinical Cancer Research : An Official Journal of the American Association for Cancer Research*, *8*(4), 1172–1181.

Perlman, M., & Resh, M. D. (2006). Identification of an intracellular trafficking and assembly pathway for HIV-1 gag. *Traffic (Copenhagen, Denmark)*, *7*(6), 731–745. https://doi.org/10.1111/j.1398-9219.2006.00428.x

Pokorski, J. K., & Steinmetz, N. F. (2011). The art of engineering viral nanoparticles. *Molecular Pharmaceutics*, *8*(1), 29–43. https://doi.org/10.1021/mp100225y

Puente-Massaguer, E., Grau-Garcia, P., Strobl, F., Grabherr, R., Striedner, G., Lecina, M., & Gòdia, F. (2021). Accelerating HIV-1 VLP production using stable High Five insect cell pools. *Biotechnology Journal*, *16*(4), e2000391. https://doi.org/10.1002/biot.202000391

Pumpens, P., & Grens, E. (2002). Artificial Genes for Chimeric Virus-Like Particles. In *Artificial DNA* (Issue February). https://doi.org/10.1201/9781420040166.ch8

Reid, A., Vidal, L., Shaw, H., & de Bono, J. (2007). Dual inhibition of ErbB1 (EGFR/HER1) and ErbB2 (HER2/neu). *European Journal of Cancer (Oxford, England : 1990)*, *43*(3), 481–489. https://doi.org/10.1016/j.ejca.2006.11.007

Roh, H., Hirose, C. B., Boswell, C. B., Pippin, J. A., & Drebin, J. A. (1999). Synergistic antitumor effects of HER2/neu antisense oligodeoxynucleotides and conventional chemotherapeutic agents. *Surgery*, *126*(2), 413–421.

Roh, H., Pippin, J., & Drebin, J. A. (2000). Down-regulation of HER2/neu expression induces apoptosis in human cancer cells that overexpress HER2/neu. *Cancer Research*, *60*(3), 560–565.

Rusnak, D. W., Affleck, K., Cockerill, S. G., Stubberfield, C., Harris, R., Page, M., Smith, K. J., Guntrip, S. B., Carter, M. C., Shaw, R. J., Jowett, A., Stables, J., Topley, P., Wood, E. R., Brignola, P. S., Kadwell, S. H., Reep, B. R., Mullin, R. J., Alligood, K. J., … Lackey, K. (2001). The characterization of novel, dual ErbB-2/EGFR, tyrosine kinase inhibitors: potential therapy for cancer. *Cancer Research*, *61*(19), 7196–7203.

Rybicki, E. P. (2019). *Plant molecular farming of virus-like nanoparticles as vaccines and reagents*. *July*, 1–22. https://doi.org/10.1002/wnan.1587

Sanna, V., Pala, N., & Sechi, M. (2014). Targeted therapy using nanotechnology: focus on cancer. *International Journal of Nanomedicine*, *9*, 467–483. https://doi.org/10.2147/IJN.S36654

Santos, J., Cardoso, M., Moreira, I. S., Gonçalves, J., Correia, J. D. G., Verde, S. C., & Melo, R. (2021). Integrated in Silico and Experimental Approach towards the Design of a Novel Recombinant Protein Containing an Anti-HER2 scFv. *International Journal of Molecular Sciences*, *22*(7). https://doi.org/10.3390/ijms22073547

Shi, B., Xue, M., Wang, Y., Wang, Y., Li, D., Zhao, X., & Li, X. (2018). An improved method for increasing the efficiency of gene transfection and transduction. *International Journal of Physiology, Pathophysiology and Pharmacology*, *10*(2), 95–104. http://www.ncbi.nlm.nih.gov/pubmed/29755642%0Ahttp://www.pubmedcentral.nih.gov/articlerender.fcgi?artid=PMC5943608

Shirbaghaee, Z., & Bolhassani, A. (2016). Different applications of virus-like particles in biology and medicine: Vaccination and delivery systems. *Biopolymers*, *105*(3), 113–132. https://doi.org/10.1002/bip.22759

Steinmetz, N. F. (2010). Viral nanoparticles as platforms for next-generation therapeutics and imaging devices. In *Nanomedicine: Nanotechnology, Biology, and Medicine* (Vol. 6, Issue 5, pp. 634–641). NIH Public Access. https://doi.org/10.1016/j.nano.2010.04.005

Tai, W., Mahato, R., & Cheng, K. (2010). The role of HER2 in cancer therapy and targeted drug delivery. *Journal of Controlled Release : Official Journal of the Controlled Release Society*, *146*(3), 264–275. https://doi.org/10.1016/j.jconrel.2010.04.009

Tan, A. R., & Swain, S. M. (2003). Ongoing adjuvant trials with trastuzumab in breast cancer. *Seminars in Oncology*, *30*(5 Suppl 16), 54–64. https://doi.org/10.1053/j.seminoncol.2003.08.008

Tedbury, P. R., & Freed, E. O. (2014). The role of matrix in HIV-1 envelope glycoprotein incorporation. *Trends in Microbiology*, *22*(7), 372–378. https://doi.org/10.1016/j.tim.2014.04.012

Tolmachev, V., Orlova, A., Pehrson, R., Galli, J., Baastrup, B., Andersson, K., Sandström, M., Rosik, D., Carlsson, J., Lundqvist, H., Wennborg, A., & Nilsson, F. Y. (2007). Radionuclide therapy of HER2-positive microxenografts using a 177Lu-labeled HER2-specific Affibody molecule. *Cancer Research*, *67*(6), 2773–2782. https://doi.org/10.1158/0008-5472.CAN-06-1630

Visciano, M. L., Diomede, L., Tagliamonte, M., Tornesello, M. L., Asti, V., Bomsel, M., Buonaguro, F. M., Lopalco, L., & Buonaguro, L. (2011). Generation of HIV-1 Virus-Like Particles expressing different HIV-1 glycoproteins. *Vaccine*, *29*(31), 4903–4912. https://doi.org/10.1016/j.vaccine.2011.05.005

Wang, J. W., & Roden, R. B. S. (2013). Virus-like particles for the prevention of human papillomavirus-associated malignancies. *Expert Review of Vaccines*, *12*(2), 129–141. https://doi.org/10.1586/erv.12.151

Wang, N., Chen, M., & Wang, T. (2019). Liposomes used as a vaccine adjuvant-delivery system: From basics to clinical immunization. *Journal of Controlled Release : Official Journal of the Controlled Release Society*, *303*, 130–150. https://doi.org/10.1016/j.jconrel.2019.04.025

Wang, T., Larcher, L. M., Ma, L., & Veedu, R. N. (2018). Systematic Screening of Commonly Used Commercial Transfection Reagents towards Efficient Transfection of Single-Stranded Oligonucleotides. *Molecules (Basel, Switzerland)*, *23*(10). https://doi.org/10.3390/molecules23102564

Wang, Y., Zhang, Y., Yu, Y., Ren, L., Wang, J., Cheng, L., Jiang, D., Guo, X., Teng, T., Luo, X., Lv, S., Wang, X., Wang, H., Shi, X., Zhang, H., & Bi, S. (2020). Preparation and preliminary evaluation of hepatitis B core antigen virus like nanoparticles loaded with indocyanine green. *Annals of Translational Medicine*, *8*(24), 1661. https://doi.org/10.21037/atm-20-7478

Yan, D., Wei, Y.-Q., Guo, H.-C., & Sun, S.-Q. (2015). The application of virus-like particles as vaccines and biological vehicles. *Applied Microbiology and Biotechnology*, *99*(24), 10415–10432. https://doi.org/10.1007/s00253-015-7000-8

Yang, G., Cai, K. Q., Thompson-Lanza, J. A., Bast, R. C. J., & Liu, J. (2004). Inhibition of breast and ovarian tumor growth through multiple signaling pathways by using retrovirus-mediated small interfering RNA against Her-2/neu gene expression. *The Journal of Biological Chemistry*, *279*(6), 4339–4345. https://doi.org/10.1074/jbc.M311153200

Yoon, V., Fridkis-Hareli, M., Munisamy, S., Lee, J., Anastasiades, D., & Stevceva, L. (2010). The GP120 molecule of HIV-1 and its interaction with T cells. *Current Medicinal Chemistry*, *17*(8), 741–749. https://doi.org/10.2174/092986710790514499

Zdanowicz, M., & Chroboczek, J. (2016). Virus-like particles as drug delivery vectors. *Acta Biochimica Polonica*, *63*(3), 469–473. https://doi.org/10.18388/abp.2016_1275

Zeltins, A. (2013). Construction and characterization of virus-like particles: a review. *Molecular Biotechnology*, *53*(1), 92–107. https://doi.org/10.1007/s12033-012-9598-4

Ziada, A., Barqawi, A., Glode, L. M., Varella-Garcia, M., Crighton, F., Majeski, S., Rosenblum, M., Kane, M., Chen, L., & Crawford, E. D. (2004). The use of trastuzumab in the treatment of hormone refractory prostate cancer; phase II trial. *The Prostate*, *60*(4), 332–337. https://doi.org/10.1002/pros.20065

6. Annexes

Plasmid Maps

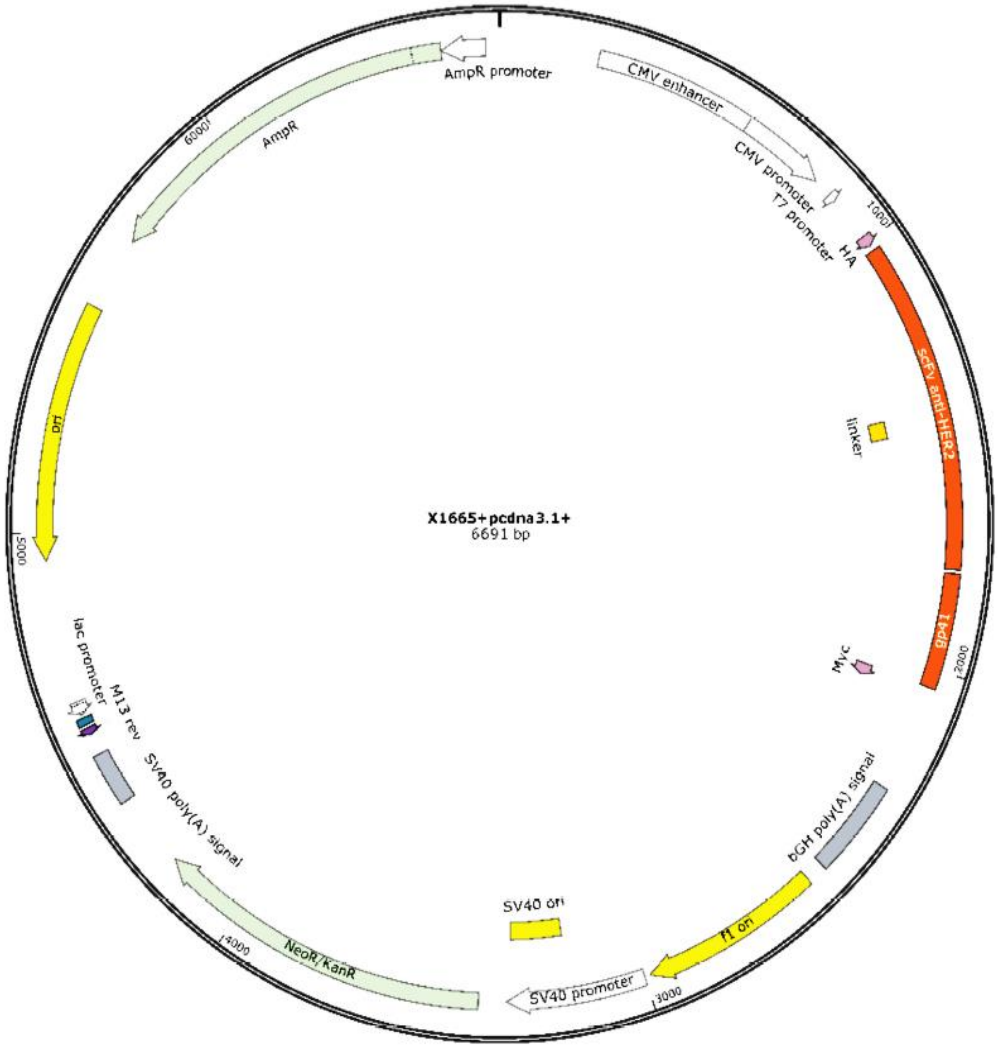

Figure A 1: Features and genomic map of X1665+pcDNA3.1+.

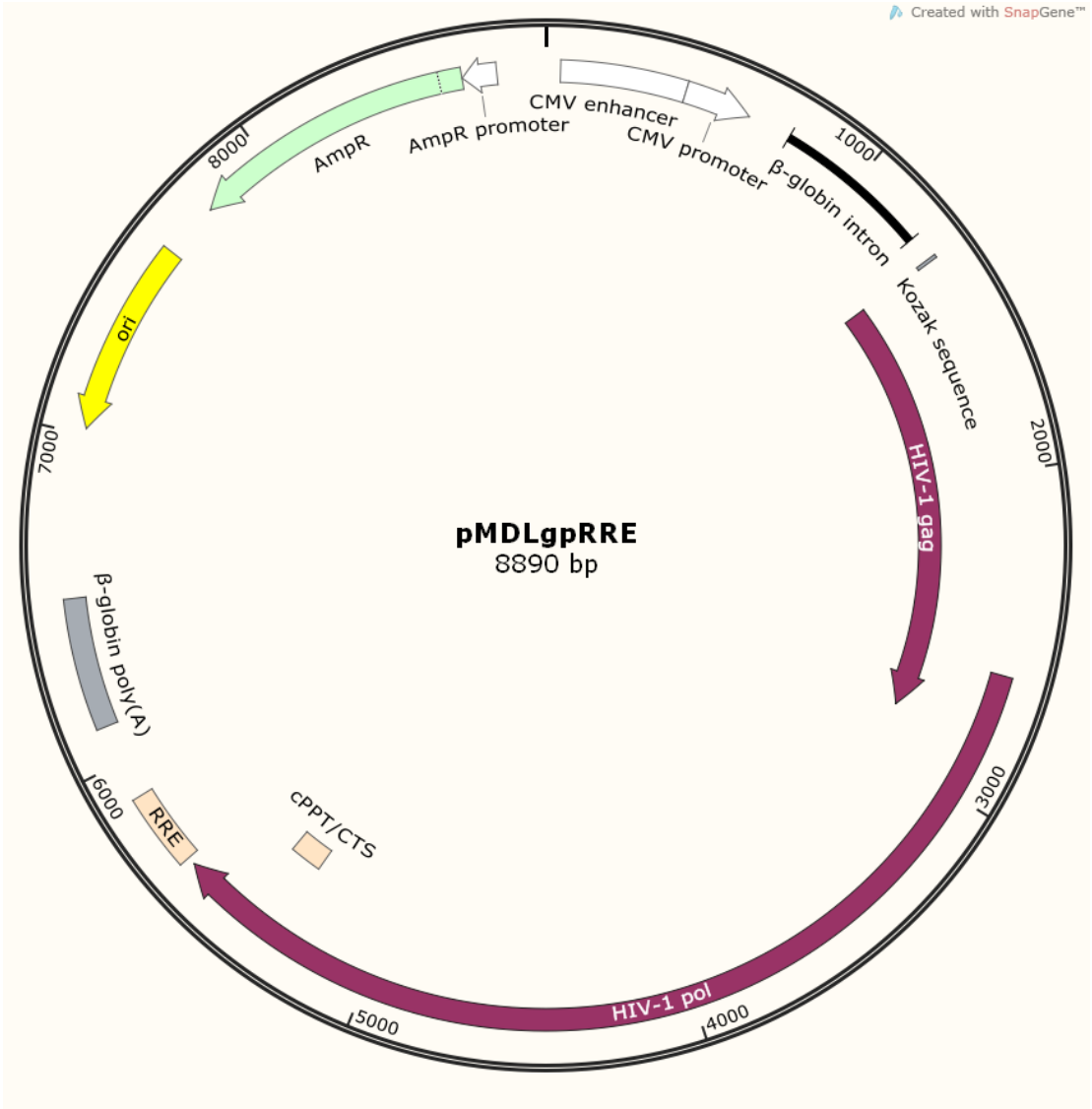

Figure A 2: Features and genomic map of pMDLg/pREE.

Figure A 3: Features and genomic map of pRSV-REV.

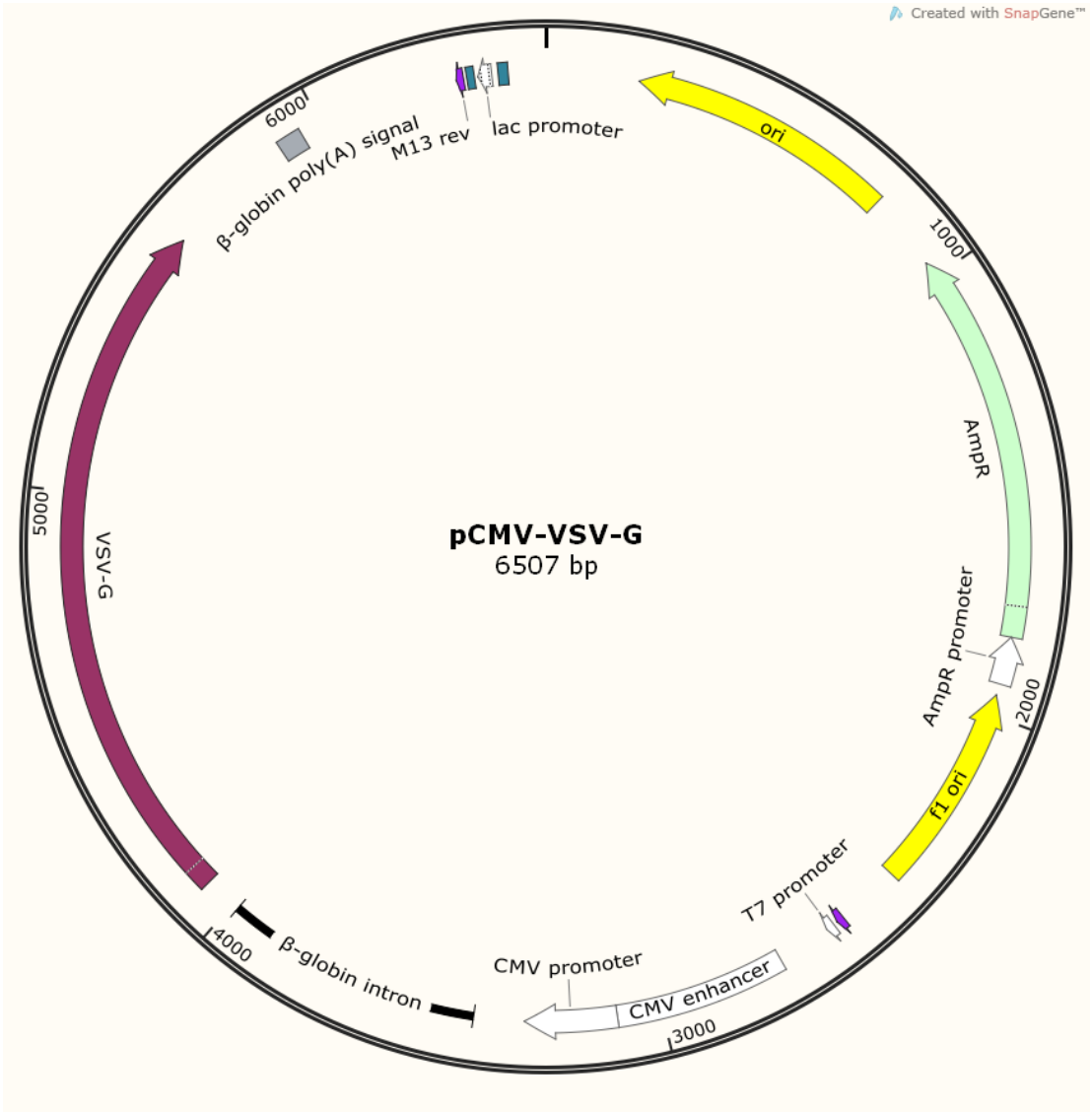

Figure A 4: Features and genomic map of pCMV-VSV-G.

Figure A 5: Features and genomic map of pHR_EGFPligang.